Increased Abundance of Proteins Involved in Phytosiderophore Production in Boron-Tolerant Barley[1][C][W]

John Patterson*, Kris Ford, Andrew Cassin, Siria Natera, and Antony Bacic

Australian Centre for Plant Functional Genomics, School of Botany, University of Melbourne, Victoria, Australia, 3010

Boron (B) phytotoxicity affects cereal-growing regions worldwide. Although B-tolerant barley (*Hordeum vulgare*) germplasm is available, molecules responsible for this tolerance mechanism have not been defined. We describe and use a new comparative proteomic technique, iTRAQ peptide tagging (iTRAQ), to compare the abundances of proteins from B-tolerant and -intolerant barley plants from a 'Clipper' × 'Sahara' doubled-haploid population selected on the basis of a presence or absence of two B-tolerance quantitative trait loci. iTRAQ was used to identify three enzymes involved in siderophore production (Iron Deficiency Sensitive2 [IDS2], IDS3, and a methylthio-ribose kinase) as being elevated in abundance in the B-tolerant plants. Following from this result, we report a potential link between iron, B, and the siderophore hydroxymugineic acid. We believe that this study highlights the potency of the iTRAQ approach to better understand mechanisms of abiotic stress tolerance in cereals, particularly when applied in conjunction with bulked segregant analysis.

Boron (B) is an essential plant micronutrient but is toxic at high levels. Elevated soil B is a common feature of soils derived from marine sediments, a feature of the geological history of many cereal-growing regions in Australia. B phytotoxicity also affects soils in North Africa and western Asia. In barley (*Hordeum vulgare*), yield penalties of up to 17% have been attributed directly to B phytotoxicity (Cartwright et al., 1984). A number of barley accessions, originally isolated from northern Africa, display striking B tolerance (Nable, 1988), and incorporation of these B-tolerance traits into elite barley varieties continues to be part of current breeding programs.

A genetic study examining B toxicity tolerance in barley identified four quantitative trait loci (QTL) contributing to B tolerance (Jeffries et al., 1999). The two strongest QTL were on chromosomes 4H and 6H, and both contribute to a net reduction in B uptake (Jeffries et al., 1999). Thus, although multiple mechanisms may be involved in the reduction of B accumulation in planta, the actual molecular entities that are encoded by the 4H and 6H QTL are unknown. The mechanism(s) appears to be constitutive, with tolerant plants accumulating less B compared to intolerant varieties, regardless of the external B concentration (Nable, 1988; Hayes and Reid, 2004). Following from these previous studies, any mechanism leading to a reduced B uptake in both the roots and the leaves would necessarily have to function at the site of B uptake, namely at the plasma membrane (PM) of cells at the root epidermis.

The involvement of an anion transporter responsible for B efflux has recently been predicted (Hayes and Reid, 2004), although the identity of this protein is unknown. PM-located proteins with both active and passive B-transporting roles have been identified in Arabidopsis (*Arabidopsis thaliana*; Bor1 [Takano et al., 2002] and NIP5;1 [Takano et al., 2006]), but no B transporter has been demonstrated to be involved in a B-tolerance mechanism. B also has a capacity to form complexes with a variety of hydroxylated molecules (Power and Woods, 1997), most notably in the cell wall, where B is involved in complexing molecules of rhamnogalactouranan II via ester linkages to apiosyl residues (O'Neill et al., 2004). Given the conditions for B-rhamnogalactouranan II complexation exist in the apoplast, other B complexes may also be formed in this region and cannot currently be excluded from an involvement in a B-tolerance mechanism.

Regardless of how B tolerance occurs in planta, it is likely that differences in proteins, either in relative levels or amino acid sequence, will play a key role. Proteins involved in the regulation of membrane-bound transporters, as well as those involved in the synthesis of many low M_r hydroxylated metabolites, reside in the cytoplasm. With this information in mind, we decided to compare the soluble, cytoplasmic proteins

[1] This work was supported by the Australian Research Council, the Grain Research and Development Corporation, and the Victorian and South Australian State Governments.

* Corresponding author; e-mail johnhp@unimelb.edu.au; fax 61–3–9347–1071.

The author responsible for distribution of materials integral to the findings presented in this article in accordance with the policy described in the Instructions for Authors (www.plantphysiol.org) is: John Patterson (johnhp@unimelb.edu.au).

[C] Some figures in this article are displayed in color online but in black and white in the print edition.

[W] The online version of this article contains Web-only data.

www.plantphysiol.org/cgi/doi/10.1104/pp.107.096388

isolated from the roots of B-tolerant and B-intolerant plants using a quantitative mass spectrometry (MS) approach.

Following the first descriptions of multidimensional peptide chromatography and MS/MS identification (MudPIT) by Yates and colleagues (Washburn et al., 2001), this approach has been rapidly adopted in the plant field as an approach to identify hundreds of proteins from a single sample (Zieske, 2006). A limitation of the current techniques has been the difficulty of performing quantitative comparisons between multiple samples from separate experiments. Recently, a series of isobaric peptide tags (iTRAQ, Applied Biosystems) has allowed the comparative, quantitative analysis of up to four samples in a single MudPIT-style experiment. The chemically identical but isotopically distinct iTRAQ tags are attached to peptides through amine groups prior to pooling samples and analyzing by MS/MS (Fig. 1A). Due to the identical chemistry of the distinct tags, identical peptides (with MS differentiable tags) will coelute into the mass spectrometer during peptide fractionation. During MS/MS peptide fragmentation, ions derived from the distinct tags are detected, with the relative intensities of the different tags corresponding to the relative abundances of the peptides in the different samples (Fig. 1B).

In this study, we describe application of iTRAQ technology to the analysis of soluble proteins isolated from hydroponically grown barley plants. Initially, we tested the system by comparing two pools of proteins isolated from the leaves of replicate barley 'Golden Promise' plants. This allowed us to establish that the methodology was robust and sufficiently sensitive to detect small changes (>2.5-fold) in protein abundances between samples. We then used iTRAQ to look for differences in protein abundances between two pools of genetically similar barley plants that are defined by the presence or absence of both the 4H and 6H B-tolerance loci.

Few previous studies have examined the differences in proteins found in different tissues in barley plants. We found little overlap in the proteins identified from the soluble pools of proteins from the roots and leaves of barley plants, ignoring the varietal differences between the two analyses. Unsurprisingly, the soluble protein complement of both tissues was dominated by enzymes involved in metabolic processes in both tissues. Four proteins showed an increase in abundance in the B-tolerant plants. Three of these proteins are involved in production of phytosiderophores, and all four proteins have previously been demonstrated to be increased in expression in response to iron (Fe)

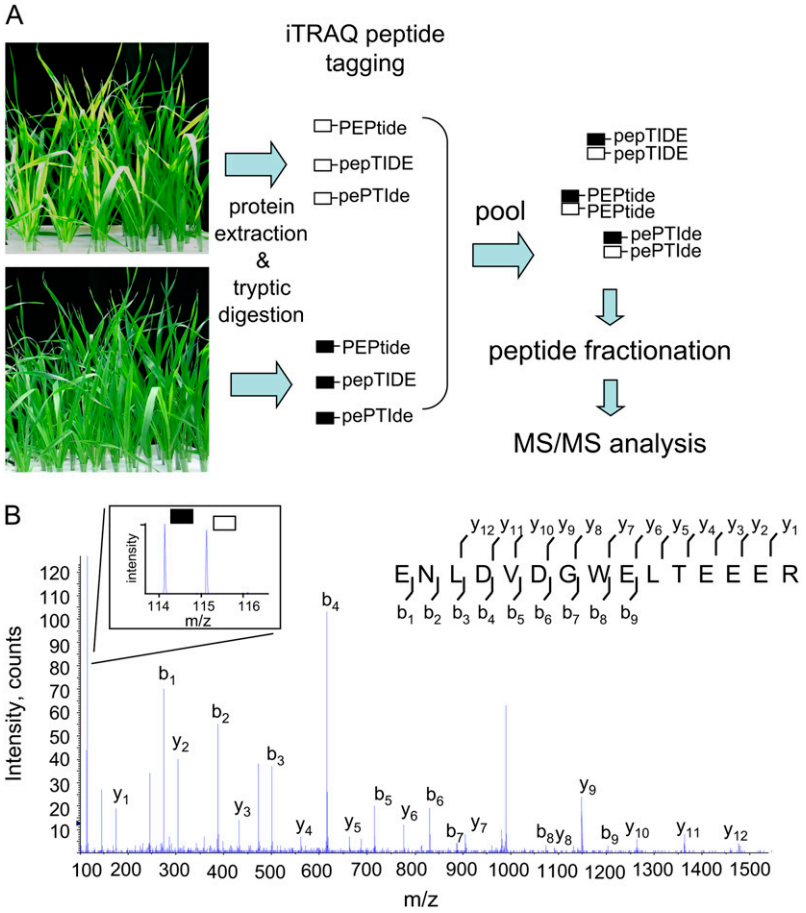

Figure 1. iTRAQ peptide tagging. A, Flow diagram outlining major steps of workflow leading to the comparative analysis of peptide abundances between samples using iTRAQ peptide tagging. In this example, proteins are extracted from two pools of plants and independently digested. Each pool of peptides is labeled with different iTRAQ tags; in this example, black (*m/z* 114) and white (*m/z* 115) are used. After tagging, the samples were pooled. Due to the identical chemistry of the tags, identical peptides from different samples cofractionate and are eluted into and analyzed by the MS simultaneously. B, Representative MS/MS spectra of iTRAQ-tagged peptide. MS/MS spectra of iTRAQ-tagged peptide matching to TC14799, NADH-dependent oxidoreductase. y and b ions are labeled. Inset, An expanded view of reporter ion region. This peptide is present in relatively similar abundances in both samples, as evidenced by the similar peak areas of reporter ions *m/z* 114 (black) and *m/z* 115 (white). [See online article for color version of this figure.]

deficiency (Negishi et al., 2002). Two of these proteins catalyze the final two steps in the synthesis of the phytosiderophore hydroxymugineic acid (HMA), while the third is involved in the Yang (Met) cycle, which provides *S*-adenosyl Met (SAM) for HMA production (Mori and Nishizawa, 1987). A possible role for this compound in B tolerance is discussed.

RESULTS

Identification of Proteins from the Leaves of 'Golden Promise' Barley Plants

Initially, we examined the variation of the iTRAQ system by comparing the abundances of proteins isolated from the leaves of replicate 'Golden Promise' plants. These samples were independently isolated, digested, and labeled with iTRAQ tags mass-to-charge ratio (m/z) 114 and m/z 115. The pools of differentially labeled peptides were combined, fractionated, and analyzed by electrospray ionization (ESI)-MS/MS. A total of 641 peptides were identified after searching the MS/MS spectra against a six-frame translation of the barley gene indices The Institute for Genomic Research (TIGR) database (V9.0). The complete data set is presented in Supplemental Table S1.

This experiment resulted in the identification of 138 unique proteins, which are listed in Table I. Functional classification of these proteins demonstrated that they were dominated by proteins involved in metabolism (primary and secondary, 58%; Fig. 2B). Eight proteins directly involved in photosynthetic reactions, large and small subunits of Rubisco, two Rubisco activase isoforms, two (23 and 33 kD) oxygen-evolving PSII proteins, and two plastocyanins (including a blue copper-binding protein) were identified, highlighting photosynthesis as one of the dominant metabolic processes occurring in green tissue. Proteins involved in translation (five elongation factors and five ribosomal proteins) and protein folding (including seven heat shock proteins) also made up 16% of the identifications, indicating that protein synthesis was also a major process occurring in this tissue. A small percentage of proteins (6%) were classified as unknown due to a lack of a predicted function.

The distribution of numbers of peptides defining a family is shown in Supplemental Figure S1 (white bars). Over 75% of the protein matches included at least three peptides with two proteins, phosphoglycerate kinase, and the large subunit of Rubisco, defined by a large number of peptides (20 and 15, respectively; Table I).

Defining the Variation within the Experimental System

The second aspect of this analysis was the comparison of relative peptide abundances between the two pools of proteins isolated from the replicate plants. iTRAQ ratios were collected for 480 of the 641 peptides (74%). The distribution of these iTRAQ ratios is shown in Figure 2A, with peak area data shown in Supplemental Figure S2. Over 50% of the peptides displayed a variation between pools of less than 0.25-fold from the median (black box), and 80% of the ratios deviated less than 0.5-fold from the median (Fig. 2A). Of the 480 peptides, 19 (3.96%) had ratios that were more than 2.5-fold different between the replicate samples.

Three extreme outliers were apparent in this data set (Fig. 2A, asterisks). The two peptides with the largest ratios of 0.53 and 0.41 (indicating an increase in peptide abundance of 3.38 and 2.57, respectively, in one sample) were derived from the small and large subunits of Rubisco, respectively. Both subunits had multiple peptides with average iTRAQ ratios, excluding the outlying values of 0.09 (small subunit, $n = 5$) and 0 (large subunit, $n = 14$). The peptide with the lowest ratio of -0.77 was derived from Met synthase 1 (METS1); three other peptides from the same protein had an average iTRAQ ratio of -0.21. There were 16 other peptides with ratios between -0.4 and -0.6; in each of these cases, the average ratio of the other peptides that matched to the same proteins deviated by less than 0.2 units from zero (i.e. less than 1.5-fold difference). Based on this information, we decided that peptides with ratios of at least 0.4 units either side of zero (i.e. 2.5-fold difference between samples) would be selected for further examination in the subsequent analysis.

Selection of Lines Containing 4H/6H B-Tolerance Loci from the 'Clipper' × 'Sahara' Doubled-Haploid Population

In the B-tolerant barley 'Sahara,' four distinct QTL have been described that are involved in contributing to B tolerance (Jeffries et al., 1999). Two of these QTL, located on chromosomes 4H and 6H, are both linked to a reduction in B uptake. Reduced B uptake appears to be a constitutive trait, with 'Sahara' plants also accumulating less B at low concentrations of B (Nable et al., 1990).

The QTL mapping was performed using a doubled-haploid (DH) population, created from parental 'Sahara' and the B-intolerant 'Clipper.' These parental lines are distantly related and display distinct growth habits (Roessner et al., 2006). Specifically looking at root morphology, which is the site of B uptake, the 'Sahara' plants have distinctly shorter and thicker roots than the elongated, thin roots of the 'Clipper' plants (compare Fig. 3, A and B).

A comparative analysis specifically examining B tolerance would be compounded by the large varietal variation between 'Clipper' and 'Sahara.' To circumvent this, we have adopted a bulked segregant approach (Michelmore et al., 1991), exploiting the availability of a population of 150 DH lines created from crossing the B-tolerant landrace 'Sahara 3771' and the intolerant, improved 'Clipper' (Karakousis et al., 2003).

In this study, we selected two pools of plants from the DH population, each composed of 20 lines. The

Table I. *List of proteins identified from leaves isolated from 'Golden Promise' seedlings*

Proteins are ordered according to functional classification. A pie chart based on percentages represented by each functional group is presented in Figure 2B. Bold entries indicate protein also identified in root tissue.

TIGR Accession	No. of Peptides Defining Group	NCBInr	Annotation	Organism	E Value
Primary metabolism					
TC130714	8	gi|125580	Phosphoribulokinase	Wheat	0
TC131346	7	gi|62732953	Fru-bisphosphate aldolase class I	Rice	0
TC131467	3	gi|34911932	NADP-specific isocitrate dehydrogenase	Rice	0
TC131518	5	gi|29367547	Adenosine kinase-like protein	Rice	0
TC131556	4	gi|1143500	ADP-Glc pyrophosphorylase small subunit	Barley	0
TC132023	4	gi|21741	Fru-bisphosphatase	Wheat	0
TC132350	4	gi|2105137	ADP-Glc pyrophosphorylase large subunit	Barley	0
TC138581	6	gi|33113259	Enolase	Rice	0
TC138582	9	gi|763035	Glyceraldehyde-3-P dehydrogenase	*Zea mays*	0
TC138635	13	gi|108705993	Glyceraldehyde-3-P dehydrogenase B	Rice	0
TC138641	15	gi|31087909	Rubisco large subunit	Barley	0
TC138666	15	gi|167097	Ribulose 1,5-bisphosphate carboxylase activase isoform 2	Barley	0
TC146737	6	gi|167095	Ribulose 1,5-bisphosphate carboxylase activase	Barley	0
TC139062	11	gi|50934283	Glycolate oxidase	Rice	0
TC139210	4	gi|1212996	UDP-Glc pyrophosphorylase	Barley	0
TC139211	5	gi|50904581	Hydroxypyruvate reductase	Rice	0
TC139220	3	gi|77548686	Pyruvate kinase	Rice	0
TC139256	12	gi|77554291	Rubisco subunit binding-protein α-subunit	Rice	0
TC146378	20	gi|3293043	Phosphoglycerate kinase	Wheat	0
TC146528	3	gi|56785335	Phosphoglycerate mutase	Rice	0
TC146663	12	gi|28190676	Transketolase	Rice	0
TC146784	6	gi|18076790	Phosphoglucomutase	Wheat	0
TC146896	9	gi|14265	Sedoheptulose-1,7-bisphosphatase	Wheat	0
TC131363	1	gi|18978	Glyceraldehyde 3-P dehydrogenase	Barley	0
TC131622	3	gi|76363515	Fru-1,6-bisphosphatase	*Saccharum* sp.	1E-178
TC131870	1	gi|50899346	Enoyl-acyl carrier protein reductase	Rice	2E-178
TC131364	11	gi|729003	Carbonic anhydrase	Barley	3E-176
TC139061	8	gi|50934283	Glycolate oxidase	Rice	1E-172
TC139042	5	gi|21844	33-kD oxygen-evolving protein of PSII	Wheat	5E-170
TC146536	4	gi|50910187	Glyceraldehyde-3-P dehydrogenase	Rice	4E-169
TC147698	4	gi|54291349	PSII stability/assembly factor HCF136	Rice	9E-168
TC146289	5	gi|34915204	Glyoxysomal malate dehydrogenase	Rice	2E-152
TC138805	8	gi|609262	Triosephosphate isomerase	*Secale cereale*	7E-146
TC147935	3	gi|51535181	Fructokinase	Rice	3E-143
TC146529	4	gi|50932771	Malate dehydrogenase	Rice	9E-139
TC131409	3	gi|2507469	Triosephosphate isomerase	Barley	1E-120
TC131384	3	gi|15240250	Ribulose-P 3-epimerase	Arabidopsis	8E-119
TC131383	4	gi|21837	23-kD oxygen evolving protein of PSII	Wheat	6E-118
TC140560	4	gi|50934597	Rib-5-P isomerase	Rice	7E-115
TC132198	3	gi|51090360	Fru-bisphosphate aldolase	Rice	2E-108
TC138580	7	gi|11990897	Rubisco small subunit	Wheat	6E-98
TC132200	1	gi|51090360	Fru-bisphosphate aldolase	Rice	1E-77
TC134951	1	gi|56784876	Phosphoribulokinase/uridine kinase-like	Rice	4E-76
TC134990	1	gi|18978	Glyceraldehyde 3-P dehydrogenase	Barley	1E-56
TC147083	1	gi|37651973	Blue copper-binding protein	Barley	1E-54
TC146310	1	gi|431920	Plastocyanin	Barley	9E-51
TC139192	1	gi|431920	Plastocyanin	Barley	3E-50
Secondary metabolism					
TC130720	3	gi|68655441	AdoMet synthase 2	Barley	0
TC130859	**4**	**gi|34915052**	**Ferredoxin-nitrite reductase**	**Rice**	**0**
TC131827	3	gi|50082771	Hydroxymethylbutenyl 4-diphosphate synthase	*Z. mays*	0
TC139066	4	gi|417745	Adenosylhomocysteinase	Wheat	0
TC139106	4	gi|52353541	Ketol-acid reductoisomerase	Rice	0
TC139229	3	gi|1705612	Catalase isozyme 1	Barley	0

(*Table continues on following page.*)

Table I. (*Continued from previous page.*)

TIGR Accession	No. of Peptides Defining Group	NCBInr	Annotation	Organism	E Value
TC146718	4	gi|2493543	Catalase 1	Wheat	0
TC139584	3	gi|52077207	Monodehydroascorbate reductase	Rice	0
TC139836	4	gi|34894800	Dihydrolipoamide dehydrogenase	Rice	0
TC146253	7	gi|50947367	Putative aminotransferase	Rice	0
TC131070	**3**	**gi|34911282**	**Guanine nucleotide-binding protein β-subunit-like protein**	**Rice**	**3E-170**
TC138583	3	gi|32352138	Thiamine biosynthetic enzyme	Rice	7E-167
TC132431	1	gi|19849543	Porphobilinogen deaminase	Wheat	8E-166
TC139562	1	gi|55233175	β-Cyano-Ala synthase	Rice	3E-159
TC133238	3	gi|7619802	Putative glyoxalase I	Wheat	6E-158
TC131549	2	gi|3688398	Ascorbate peroxidase	Barley	1E-141
TC139685	3	gi|50909553	γ Hydroxybutyrate dehydrogenase	Rice	2E-141
TC132418	6	gi|52076371	Oxidoreductase like	Rice	1E-138
TC132249	7	gi|50945155	Oxidoreductase, Zn binding	Rice	3E-132
TC146831	8	gi|15808779	Ascorbate peroxidase	Barley	8E-128
TC146265	4	gi|28059599	Thylakoid lumenal 17.4-kD protein	Arabidopsis	4E-52
Amino acid metabolism					
TC130708	7	gi|2565305	Gly decarboxylase P subunit	Triticeae	0
TC131380	**6**	**gi|68655495**	**METS1 enzyme**	**Barley**	**0**
TC131397	9	gi|50918513	Gly hydroxymethyltransferase	Rice	0
TC131957	5	gi|1707878|	Aminomethyltransferase	*Solanum tuberosum*	0
TC139279	10	gi|50510140	Ferredoxin-dependent Glu synthase	Rice	0
TC139283	4	gi|71362640	Plastid Gln synthetase isoform GS2c	Wheat	0
TC139989	4	gi|37703720	Aminotransferase AGD2	Rice	0
TC140047	3	gi|633095	Plastidic Asp aminotransferase	*Panicum miliaceum*	0
TC146244	11	gi|50510015	Ala aminotransferase	Rice	0
TC147191	5	gi|50915564	Leu aminopeptidase	Rice	0
TC147233	7	gi|1170029	Glu-1-semialdehyde 2,1-aminomutase	Barley	0
TC146634	4	gi|585032	Cys synthase	Wheat	2E-165
TC132821	5	gi|57899533	Putative plastidic Cys synthase 1	Rice	7E-126
Carbohydrate metabolism					
TC132929	1	gi|18025340	α-L-Arabinofuranosidase/ β-D-xylosidase isoenzyme ARA-I	Barley	0
TC130915	**1**	**gi|3037080**	**Glucan endo-1,3-β-glucosidase isoenzyme I**	**Barley**	**2E-160**
Energy					
TC130729	**4**	**gi|525291**	**ATP synthase β-subunit**	Wheat	**0**
TC148629	1	gi|11583	ATPase, β-subunit	Barley	5E-60
Cytoskeleton					
TC131417	3	gi|108864035	Actin-7	Rice	0
TC146790	3	gi|1709779	Profilin-1	Barley	2E-61
Oxidative balance					
TC131399	1	gi|20302473	Ferredoxin-NADP(H) oxidoreductase	Wheat	0
TC131398	3	gi|20302471	Ferredoxin-NADP(H) oxidoreductase	Wheat	1E-167
TC130797	6	gi|34901636	Thioredoxin-like protein CDSP32	Rice	8E-111
TC130826	4	gi|3328221	Thioredoxin peroxidase	*S. cereale*	2E-109
TC131780	1	gi|6179600	GPX12Hv, glutathione peroxidase-like protein	Barley	2E-97
TC146933	4	gi|4138592	Thioredoxin M	Wheat	6E-93
TC132207	3	gi|55833012	Peroxiredoxin Q	Wheat	4E-90
TC133526	1	gi|51535721	Thioredoxin peroxidase 1	Rice	1E-79
TC131676	**4**	**gi|1572627**	**Copper/Zn superoxide dismutase**	**Wheat**	**2E-78**
TC146752	3	gi|108708142	Superoxide dismutase 1	Rice	4E-74
Defense					
TC138584	4	gi|50909007	Putative elongation factor 2	Rice	0
TC146252	7	gi|2119927	Translation elongation factor EF-G	*Glycine max*	0
TC146566	3	gi|949878	Elongation factor 1-α	Barley	0
TC146710	3	gi|50906401	Elongation factor 1-γ	Rice	1E-178
TC133131	1	gi|3550485	cp33Hv	Barley	1E-149
TC140393	5	gi|56682582	Thaumatin-like protein TLP5	Barley	3E-130
TC147110	3	gi|77556660	Elongation factor TS family protein	Rice	1E-126
TC139502	5	gi|3550483	cp31BHv	Barley	4E-126
TC148742	4	gi|77556660	Elongation factor TS family protein	Rice	6E-48

(*Table continues on following page.*)

Table I. (*Continued from previous page.*)

TIGR Accession	No. of Peptides Defining Group	NCBInr	Annotation	Organism	E Value
Translation					
TC131505	5	gi|14017610	Ribosomal protein S3	Wheat	6E-132
TC147671	1	gi|50905143	Putative 50S ribosomal protein L3	Rice	4E-111
TC131976	3	gi|50917085	Ribosomal protein	Rice	3E-98
TC131434	4	gi|968902	Ribosomal protein S8	Rice	1E-84
Protein folding				Rice	
TC131557	9	gi|77554415	70-kD heat shock-related protein	Rice	0
TC131558	**9**	**gi|92870233**	**Heat shock protein Hsp70**	***Medicago truncatula***	**0**
TC138914	5	gi|77552703	Heat shock cognate 70-kD protein	Rice	0
TC138915	4	gi|108707463	Heat shock cognate 70-kD protein	Rice	0
TC139132	8	gi|34897924	Chaperonin 60 β	Rice	0
TC139483	3	gi|556673	Heat shock protein	*S. cereale*	0
TC139572	3	gi|110289207	Chaperonin CPN60-1	Rice	0
TC132470	1	gi|50945195	Peptidyl-prolyl cis-trans isomerase	Rice	0
TC146697	1	gi|34897236	60S ribosomal protein L1	Rice	3E-174
TC146605	3	gi|13925734	Cyclophilin A-2	Wheat	1E-88
TC138916	1	gi|59799993	Heat shock protein 70	*Z. mays*	7E-85
TC135924	1	gi|50948109	Immunophilin/FKBP-type peptidyl-prolyl cis-trans isomerase	Rice	1E-51
Protein degradation					
TC131728	6	gi|399213	ATP-dependent protease ATP-binding subunit	*Lycopersicon esculentum*	0
TC141753	1	gi|22331173	ATPREP1/ATZNMP; metalloendopeptidase	Arabidopsis	1E-139
TC146981	1	gi|11967891	20S proteasome α-subunit	*Z. mays*	7E-130
TC139286	3	gi|1323748	Thiol protease	Wheat	1E-86
Signaling					
TC146758	8	gi|108862567	RNA-binding protein	Rice	0
TC147198	12	gi|50910077	Translational elongation factor Tu	Rice	0
TC133717	11	gi|50935225	Putative mRNA-binding protein precursor	Rice	1E-139
TC132022	1	gi|34913270	29-kD ribonucleoprotein A	Rice	5E-88
TC138855	**1**	**|dbj|BAA02436.1|**	**Elongation factor 1 β**	**Wheat**	**7E-70**
Unknown					
TC139280	7	gi|2072727	Fd-GOGAT protein	Rice	0
TC139914	1	gi|15235282	Amino acid-binding/oxidoreductase	Arabidopsis	0
TC146506	3	gi|50925621	OSJNBa0084K20.14	Rice	3E-114
TC141769	1	gi|54290425	Unknown protein	Rice	2E-101
TC131703	3	gi|18394414	Unknown protein	Arabidopsis	1E-79
TC150479	1	gi|50947401	Unknown protein	Rice	2E-72
TC148625	5	gi|50928389	OSJNBa0086O06.22	Rice	3E-60
TC139271	1	gi|19087	Unnamed protein product	Barley	9E-43

lines in each pool were chosen on the basis of a presence or absence of both the 4H and 6H tolerance loci. Coincident with this genotypic segregation, these lines also segregated on the basis of leaf B levels after growth in elevated levels of B (Fig. 3E; Jefferies, 2000). In terms of root morphology, these two pools of plants were very similar, with a phenotype intermediate between both the parents (compare Fig. 3, C and D).

iTRAQ Comparison of Proteins Isolated from the Roots of B-Tolerant and B-Intolerant Plants

Entire root systems from the B-tolerant and B-intolerant pools of DH plants, grown at a nontoxic concentration of B (50 μM), were harvested and homogenized. Due to the aforementioned constitutive nature of the B exclusion trait, plants were grown in a nontoxic concentration of B to minimize identification of B toxicity-responsive proteins in the intolerant plants. After centrifugation of the homogenate, soluble proteins were collected in the supernatant. Both pools of proteins were digested with trypsin, and the resultant peptides were tagged with iTRAQ tags m/z 114 (B intolerant) and m/z 115 (B tolerant). A total of 1,225 peptides were identified during the comparison of the two pools of tolerant and intolerant plants. Reporter ion peak areas were collected for 1,038 of the 1,225 peptides (84%) and are presented as a box plot in Figure 4A, while relative peak area values are shown in Supplemental Figure S3. The complete set of peptides and their assignments is included in Supplemental Table S2.

A total of 341 proteins were identified in this experiment (Table II). The proteins were classified according to predicted function, and these classifications are displayed in Figure 4B. Over one-half (54%) of the

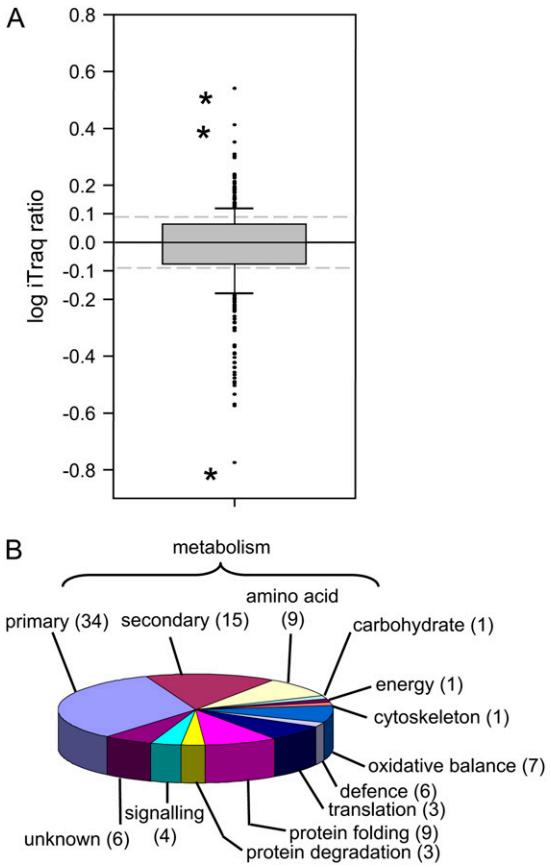

Figure 2. Relative abundance and identity of proteins identified from the leaves of barley 'Golden Promise' plants. A, Box plot showing distribution of log10-transformed iTRAQ peptide ratios derived from proteins isolated from the leaves of two identical pools of barley ('Golden Promise') plants. All 480 peptides with iTRAQ ratios are represented in this segment. Box defines the 25th and 75th percentiles of the population. Error bars define 10th and 90th percentiles of the population. Asterisks indicate extreme outlying values discussed in text. B, Pie chart showing the functional classification of the 138 unique proteins identified in this analysis. Numbers in brackets indicate the percentage of proteins within this category. [See online article for color version of this figure.]

proteins were involved in metabolic functions, including 19 proteins involved in complex carbohydrate metabolism. Ten distinct proteasome subunits were also identified. From this data set, 50 distinct proteins (representing 15% of the identifications) were identified as having no known function.

The distribution of number of peptides that define a family is shown in Supplemental Figure S1 (black bars). Less than one-half (44%) of the protein families in this experiment were defined by a single peptide that was identified using two distinct search algorithms. At the other extreme, METS1 was defined by 22 peptides, and two proteins, phosphoglycerate mutase and Phe ammonia lyase, were identified on the basis of 17 matching peptides.

Eleven of the 1,038 peptides (1.05%) had iTRAQ ratios of 0.4 (indicating 2.5-fold increase in abundance in the tolerant plants) or greater. Seven of the peptides with increased abundance in the tolerant plants could be assigned to just three proteins: a methylthio-Rib kinase (MTK), Iron Deficiency Sensitive2 (IDS2), and IDS3 (Fig. 4A). These proteins are all involved in the formation of HMA, a phytosiderophore secreted by barley plants to increase the uptake of Fe (Negishi et al., 2002). An eighth peptide was assigned to a D protein. The transcript encoding this protein has previously been identified as increasing in abundance in response to Fe deficiency (Negishi et al., 2002). The ninth peptide was assigned to a UDP-Glc-6-dehydrogenase, a protein with six other peptides also matching the amino acid sequence. The ratios of the other six peptides were

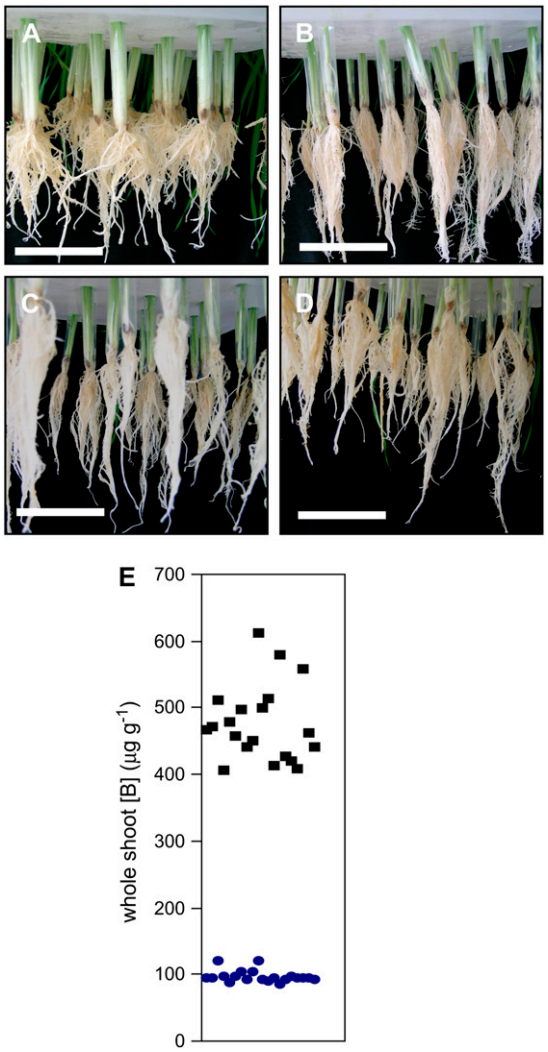

Figure 3. Photographs of roots from 2-week-old hydroponically grown plants. A, Barley 'Sahara.' B, Barley 'Clipper.' C, Representative plants from B-tolerant bulks. D, Representative plants from B-intolerant bulks. E, B accumulation in whole shoots for individual DH lines used in this study. Square symbols, intolerant lines; circles, tolerant lines. Each data point represents the whole shoot B concentration ($\mu g\ g^{-1}$) for an individual DH line used in the bulked segregant analysis, measured as described in Jeffries et al. (1999) and reproduced with permission from Jeffries (2000). Bar = 10 cm. [See online article for color version of this figure.]

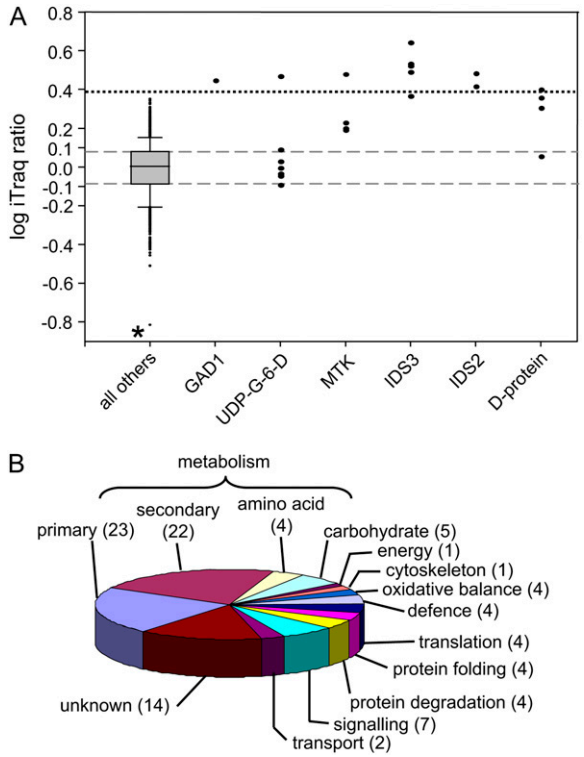

Figure 4. Relative abundance and identity of proteins identified in B-tolerant and B-intolerant plants. A, Box plots showing distribution of log-transformed iTRAQ peptide ratios derived from proteins isolated from the roots of B-tolerant and B-intolerant bulked segregants. All 1,038 peptides with iTRAQ ratios are represented in this segment. Positive values (in segment B) indicate an increase in peptide/protein abundance in the B-tolerant plants. Box defines the 25th and 75th percentiles of the population. Error bars define 10th and 90th percentiles of the population. Asterisk indicates extreme outlying values discussed in text. Dashed lines indicate values less than 0.25-fold different between samples. Dotted line indicates 2.5-fold significant difference between samples. GAD1, TC131033; UDP-G-6-D, UDP-Glc-6-dehydrogenase (TC138934); MTK, TC140103; IDS3, TC142112; IDS2 (TC137786); D-protein (TC134738). B, Pie chart showing the functional classification of the 341 proteins identified in this analysis. Numbers in brackets indicate the percentage of proteins that are present in each category. [See online article for color version of this figure.]

close to 0 (Fig. 4A). The 10th peptide with elevated abundance in the B-tolerant plants was assigned to a Glu decarboxylase, GAD1 (Glu decarboxylase isozyme1), a protein responsible for the synthesis of γ-aminobutyrate. One peptide with a negative iTRAQ ratio of 0.153 (Fig. 4A, asterisk) was derived from an *O*-methyltransferase (TC146961). This protein was identified on the basis of three peptides in total, one lacking a valid iTRAQ ratio and the other having an iTRAQ ratio of 0.94. Aside from this peptide, there were no other peptides displaying a significant decrease in the B-tolerant plants.

Plant Fe Status and B Uptake

The identification of elevated levels of proteins involved in Fe acquisition in the B-tolerant plants led us to examine if there was a relationship between Fe and B in planta. 'Clipper' and 'Sahara' plants were grown in Fe-deficient conditions, and we examined how B and zinc (Zn) accumulation in the oldest leaf and Fe accumulation in the youngest leaf was affected, using inductively coupled plasma-optical emission spectrometry.

'Sahara' plants accumulated slightly more Fe than 'Clipper' plants in both Fe-replete and Fe-depleted conditions (Fig. 5A). In 'Clipper,' Fe deficiency resulted in accumulation of similar amounts of B initially, although after 110 h, less B accumulated in the Fe-deficient plants (Fig. 5B). The opposite effect was observed in 'Sahara' plants. Compared to Fe-replete plants, Fe-deficient 'Sahara' plants accumulated significantly more B, with the difference apparent after 48 h (Fig. 5C). Fe deficiency also had a significant effect on the rate of Zn accumulating in the oldest leaves in both cultivars compared to the Fe-replete plants (Fig. 5D).

Siderophore Analysis

Siderophores were collected from the root secretions of 'Clipper' and 'Sahara' plants grown in low Fe conditions, which are known to result in elevated siderophore production (Negishi et al., 2002). Both cultivars produced deoxymugineic acid and mugineic acid (MA; Mori and Nishizawa, 1987; Fig. 6). In addition to these two compounds, 'Sahara' plants produced HMA (Fig. 6). Currently, we cannot determine if the HMA species produced in the 'Sahara' plants is the 3-hydroxy (HMA) or the 3-*epi*-hydroxy (*e*HMA) isomer.

DISCUSSION

iTRAQ and Two-Dimensional Liquid Chromatography MS/MS Analysis of Soluble Proteins Isolated from Barley

In this study, we established a comparative proteomic approach that allowed us to compare the abundances of 479 proteins from the roots and leaves of barley plants. A total of 138 of these proteins was identified from leaf tissue and 341 were identified from root tissues.

The analysis of proteins isolated from leaves of replicate 'Golden Promise' plants demonstrated that the iTRAQ approach is sufficiently sensitive to detect differences of 2.5-fold or greater between the samples under comparison. With this information in hand, protein abundances were then compared between two pools of barley plants differing in their B tolerance. Peptides with the greatest relative abundance in the B-tolerant plants, coincident with elevated abundances of greater than 2.5-fold in the tolerant plants, were all derived from proteins that had previously been demonstrated to be involved in an Fe deficiency response, with two of these proteins, IDS2 and IDS3, specifically involved in the formation of the phytosiderophore HMA.

Table II. *List of proteins identified from roots isolated from B-tolerant and B-intolerant plants*

Proteins are ordered according to functional classification. A pie chart based on percentages represented by each functional group is presented in Figure 4B. Bold entries indicate protein also found in leaf tissue.

TIGR Accession	No. of Peptides Defining Group	NCBInr	Annotation	Organism	E Value
Primary metabolism					
TC147887	5	gi|38141533	Fructan 1-exohydrolase precursor	Barley	0
TC147636	6	gi|50900276	Glc-6-P isomerase	Rice	0
TC138581	14	gi|90110845	Enolase (2-phosphoglycerate dehydratase)	Rice	0
TC147465	3	gi|2182267	Lipoxygenase	Barley	0
TC147361	4	gi|34905462	ATP citrate lyase	Rice	0
TC147336	3	gi|55847605	Suc:Suc 1-fructosyltransferase	Wheat	0
TC147154	3	gi|57900129	Transaldolase	Rice	0
TC131363	7	gi|18978	Glyceraldehyde 3-P dehydrogenase	Barley	0
TC146895	14	gi|3341490	Phospho*enol*pyruvate carboxylase	Wheat	0
TC146849	6	gi|34897872	Phosphogluconate dehydrogenase	Rice	0
TC146784	8	gi|18076790	Phosphoglucomutase	Wheat	0
TC146767	3	gi|50947901	Diphosphonucleotide phosphatase	Rice	0
TC146663	4	gi|28190676	Transketolase	Rice	0
TC146528	17	gi|56785335	Phosphoglycerate mutase	Rice	0
TC146369	10	gi|129916	Phosphoglycerate kinase	Wheat	0
TC146300	4	gi|46358940	Vacuolar invertase1	*Triticum monococcum*	0
TC139173	14	gi|2429087	Lipoxygenase 2	Barley	0
TC139815	6	gi|50912091	Diphosphate-Fru-6-P 1-phosphotransferase	Rice	0
TC139326	3	gi|52076758	Pyrophosphate-dependent phosphofructokinase	Rice	0
TC139308	7	gi|37694731	NADP malic enzyme	Rice	0
TC139301	7	gi|51091407	Aldehyde dehydrogenase	Rice	0
TC139220	8	gi|77548686	Pyruvate kinase	Rice	0
TC139210	6	gi|1212996	UDP-Glc pyrophosphorylase	Barley	0
TC139089	5	gi|94717590	GDP-Man 3,5-epimerase 2	Rice	0
TC138932	7	gi|77554940	UDP-Glc 6-dehydrogenase	Rice	0
TC133156	5	gi|4158230	Amylogenin	Wheat	0
TC132208	5	gi|50251801	Phospho*enol*pyruvate carboxylase	Rice	0
TC131693	3	gi|91694275	Glc-6-P isomerase	Barley	0
TC131518	8	gi|29367547	Adenosine kinase-like protein	Rice	0
TC131467	10	gi|34911932	NADP-specific isocitrate dehydrogenase	Rice	0
TC131388	12	gi|88687741	Suc synthase	*Lolium perenne*	0
TC149390	1	gi|49388286	Acetyl-CoA synthetase	Rice	0
TC148243	1	gi|34897074	Inosine monophosphate dehydrogenase	Rice	0
TC147295	1	gi|50920285	Rubisco subunit binding-protein α-subunit precursor	Rice	0
TC146860	1	gi|21263612	Formate dehydrogenase, mitochondrial precursor	Barley	0
TC139625	2	gi|77549262	Pyruvate kinase	Rice	0
TC139350	2	gi|8918502	Glc-6-P dehydrogenase	Rice	0
TC139062	1	gi|50934283	Glycolate oxidase	Rice	0
TC134291	1	gi|52077150	Fru/tagatose bisphosphate aldolase	Rice	0
TC132727	1	gi|6685803	Adenylosuccinate synthetase	Wheat	0
TC132006	2	gi|50912579	Pyruvate dehydrogenase E1 α-subunit	Rice	0
TC131953	1	gi|18844860	dTDP-Glc 4,6-dehydratase	Rice	0
TC131782	1	gi|34906844	Phospho-2-dehydro-3-deoxyheptonate aldolase 1	Rice	0
TC131346	1	gi|62732953	Fru-bisphosphate aldolase class I	Rice	0
TC130807	7	gi|50948183	Sorbitol dehydrogenase	Rice	2E-177
TC131237	1	gi|62130764	Hexokinase 6	Rice	4E-175
TC147925	1	gi|27817922	Transaldolase ToTAL2	Rice	2E-172
TC146609	6	gi|18202485	Malate dehydrogenase	*Z. mays*	8E-171
TC131070	**8**	**gi|1346109**	**Guanine nucleotide-binding protein β-subunit**	**Rice**	**3E-170**
TC139687	8	gi|34907582	Fructokinase I	Rice	7E-164
TC147014	11	gi|50940457	Fructokinase	Rice	2E-163
TC147086	6	gi|28950668	Legumin-like protein	*Z. mays*	3E-163
TC147455	3	gi|81686712	Glu dehydrogenase 2	Rice	1E-160
TC146537	1	gi|34911788	Malate dehydrogenase	Rice	1E-152
TC138805	5	gi|609262	Triosephosphate isomerase	*S. cereale*	7E-146
TC132870	3	gi|108706464	Hydrolase, carbon-nitrogen family protein	Rice	1E-142
TC147359	3	gi|34905462	ATP citrate lyase	Rice	4E-141

(*Table continues on following page.*)

Table II. (*Continued from previous page.*)

TIGR Accession	No. of Peptides Defining Group	NCBInr	Annotation	Organism	E Value
TC146529	3	gi|50932771	Malate dehydrogenase	Rice	9E-139
TC146498	3	gi|729003	Carbonic anhydrase	Barley	3E-136
TC147237	1	gi|17385742	D-Isomer specific 2-hydroxyacid dehydrogenase	Rice	2E-125
TC131409	8	gi|2507469	Triosephosphate isomerase	Barley	1E-120
TC139245	4	gi|28192421	Dehydroascorbate reductase	Wheat	2E-112
TC146774	4	gi|23504745	Glutathione transferase F5	Wheat	3E-106
TC132874	4	gi|50941197	Monodehydroascorbate reductase	Rice	2E-101
TC139680	4	gi|9711921	Adenine phosphoribosyltransferase	Barley	2E-96
TC133105	1	gi|38426301	6-Phosphogluconate dehydrogenase	Rice	2E-86
TC139131	3	gi|9652119	Nucleoside diphosphate kinase	*L. perenne*	6E-79
TC150725	1	gi|55773816	Ribokinase like	Rice	7E-76
TC148941	1	gi|50917631	Deoxyuridine triphosphatase	Rice	3E-72
TC146554	11	gi|18496065	Fru 1-,6-biphosphate aldolase	Wheat	5E-68
TC144012	3	gi|5052007	Apoplastic invertase	Rice	4E-59
BG309197	1	gi|50904517	UMP synthase 1	Rice	4E-55
TC147083	3	gi|37651973	Blue copper-binding protein	Barley	1E-54
TC133349	1	gi|37651973	Blue copper-binding protein	Barley	5E-40
TC147221	1	gi|6007803	D-Ribulose-5-P 3-epimerase	Rice	7E-40
CA019619	1	gi|52077150	Fru/tagatose bisphosphate aldolase	Rice	1E-36
TC142991	1	gi|37730876	Legumin-like protein	*Z. mays*	1E-26
TC144813	1	gi|50919645	AMP-binding protein	Rice	1E-13
Secondary metabolism					
TC147448	5	gi|4566505	β-D-Glucan exohydrolase isoenzyme ExoI	Barley	0
TC147311	3	gi|50401177	Met *S*-methyltransferase	Rice	0
TC147191	10	gi|50915564	Leu aminopeptidase	Rice	0
TC147167	4	gi|12407304	IDI2	Barley	0
TC146955	9	gi|2506825	Lipoxygenase 1	Barley	0
TC146875	11	gi|50941891	Aconitate hydratase	Rice	0
TC146792	9	gi|18904	Aspartic proteinase	Barley	0
TC146761	3	gi|17887465	Phosphoethanolamine methyltransferase	Wheat	0
TC142112	5	gi|9711238	IDS3	Barley	0
TC141775	4	gi|34912652	Acetyl transferase	Rice	0
TC141288	3	gi|50919455	Leukotriene A-4 hydrolase	Rice	0
TC140255	4	gi|50906357	Aminopeptidase M	Rice	0
TC140156	4	gi|34906304	Taxadien-5-α-ol *O*-acetyltransferase	Rice	0
TC140103	4	gi|46883147	MTK	Rice	0
TC139584	6	gi|52077207	Monodehydroascorbate reductase	Rice	0
TC139517	3	gi|73913047	Δ-1-Pyrroline-5-carboxylate dehydrogenase	Barley	0
TC139434	5	gi|322833	Glu-ammonia ligase	Barley	0
TC139408	4	gi|92429669	Aconitate hydratase 1	*Sorghum bicolor*	0
TC139106	3	gi|52353541	Ketol-acid reductoisomerase	Rice	0
TC138810	17	gi|50910709	Phe ammonia lyase	Rice	0
TC137786	5	gi|285634	IDS2	Barley	0
TC131815	3	gi|50948547	Aminopeptidase N	Rice	0
TC131783	6	gi|34334010	Cytosolic glutathione reductase	*T. monococcum*	0
TC131701	9	gi|50919385	Methylenetetrahydrofolate reductase	Rice	0
TC131524	7	gi|15236375	Gly hydroxymethyltransferase	Arabidopsis	0
TC131046	5	gi|68655435	AdoMet synthase 1	Barley	0
TC131477	5	gi|50659026	UDP-D-glucuronate decarboxylase	Barley	0
TC131451	3	gi|50915842	Alcohol dehydrogenase class III	Rice	0
TC147775	1	gi|63021727	12-Oxo-phytodienoic acid reductase	*Z. mays*	0
TC147691	1	gi|54290767	Dehydroquinate dehydratase	Rice	0
TC147596	2	gi|60686892	Δ 1-Pyrroline-5-carboxylate synthetase	Wheat	0
TC147044	2	gi|32400295	Hydroxyanthranilate hydroxycinnamoyl-transferase 3	*Avena sativa*	0
TC146990	1	gi|77551313	Metallopeptidase family M24-containing protein	Rice	0
TC141625	1	gi|45510867	*N*-myristoyl transferase	Wheat	0
TC139989	1	gi|37703720	Aminotransferase AGD2	Rice	0
TC139595	1	gi|15238398	Oxysterol binding (Arabidopsis)	Arabidopsis	0
TC139279	1	gi|50510140	Ferredoxin-dependent Glu synthase	Rice	0

(*Table continues on following page.*)

Table II. (*Continued from previous page.*)

TIGR Accession	No. of Peptides Defining Group	NCBInr	Annotation	Organism	E Value
TC132714	1	gi|77554110	Aspartyl aminopeptidase	Rice	0
TC132209	1	gi|77556036	Metalloenzyme superfamily	Rice	0
TC132132	1	gi|108707229	Chorismate synthase 2, chloroplast precursor	Rice	0
TC131599	1	gi|50915896	3-Ketoacyl-CoA thiolase; acetyl-CoA acyltransferase	Rice	0
TC130859	**1**	**gi|34915052**	**Ferredoxin-nitrite reductase**	**Rice**	**0**
TC139402	5	gi|50899020	Acetyl-CoA C-acyltransferase	Rice	1E-179
TC132326	1	gi|50913253	1-Aminocyclopropane-1-carboxylate deaminase	Rice	3E-179
TC142387	1	gi|29466964	Secretory acid phosphatase precursor	Rice	1E-178
TC132270	1	gi|108711425	Ferredoxin-NADP reductase, root isozyme	Rice	3E-173
TC132684	1	gi|34912654	Acetyl transferase	Rice	2E-171
TC141237	5	gi|27531337	*O*-methyltransferase	Barley	8E-168
TC131211	5	gi|50941905	Glyoxalase I	Rice	7E-156
TC131671	1	gi|50932765	Lipase	Rice	6E-155
TC140063	3	gi|45735967	41-kD chloroplast nucleoid DNA-binding protein	Rice	2E-153
TC131287	1	gi|52077048	Molybdenum cofactor sulfurase protein like	Rice	1E-147
TC141301	1	gi|50912077	NADPH-thioredoxin reductase	Rice	3E-142
TC139685	5	gi|50909553	γ Hydroxybutyrate dehydrogenase	Rice	2E-141
TC139567	3	gi|57900400	*S*-formylglutathione hydrolase	Rice	1E-137
TC146961	3	gi|62734422	*O*-methyltransferase	Rice	2E-132
TC133095	6	gi|62734422	*O*-methyltransferase	Rice	1E-129
TC130741	2	gi|50915968	Fibrillarin	Rice	2E-128
TC146831	8	gi|15808779	Ascorbate peroxidase	Barley	8E-128
TC146925	1	gi|108706322	1,2-Dihydroxy-3-keto-5-methylthiopentene dioxygenase	Rice	2E-110
TC140546	4	gi|34897892	Methylthioadenosine	Rice	2E-109
TC139390	3	gi|34909214	ADP-ribosylation factor	Rice	3E-101
TC146548	1	gi|50947279	Caffeoyl-CoA *O*-methyltransferase 1	Rice	1E-100
TC147322	4	gi|53749369	1,4-Benzoquinone reductase	Rice	2E-99
TC130725	2	gi|32401384	Cyclophilin	Wheat	2E-92
TC151803	2	gi|21212950	Glutathione-*S*-transferase, I subunit	Barley	7E-89
TC132414	1	gi|50913035	*S*-adenosyl-methionine methyltransferase	Rice	1E-88
TC150875	3	gi|50916004	*O*-diphenol-*O*-methyl transferase	Rice	3E-85
TC147986	3	gi|22022398	Glutathione-*S*-transferase Cla47	Wheat	1E-65
TC144930	1	gi|22202676	Dioxygenase extradiol	Rice	6E-65
TC146383	5	gi|51536102	Formate-tetrahydrofolate ligase	Rice	9E-58
TC131587	1	gi|54111525	Immunophilin	*Z. mays*	2E-52
TC147423	1	gi|50940931	Blue copper-binding protein	Rice	6E-39
TC143987	1	gi|50916927	Oxidoreductase	Rice	2E-33
TC137024	3	gi|21593610	Globulin-like protein	Arabidopsis	1E-21
BQ471723	1	gi|63021725	12-Oxo-phytodienoic acid reductase	*Z. mays*	3E-18
Amino acid metabolism					
TC139066	10	gi|417745	Adenosylhomocysteinase	Wheat	0
TC131380	**22**	**gi|68655495**	**METS1 enzyme**	**Barley**	**0**
TC130910	5	gi|89511843	Asp aminotransferase	Barley	0
TC130906	6	gi|57900353	Asp aminotransferase	Rice	0
TC130774	3	gi|50540685	GAD	Rice	0
TC147620	1	gi|56784224	Asp aminotransferase	Rice	0
TC140390	1	gi|50937181	β-Ala synthases	Rice	0
TC140047	1	gi|633095	Plastidic Asp aminotransferase	*P. miliaceum*	0
TC146634	7	gi|585032	Cys synthase	Wheat	2E-165
TC147456	1	gi|81686712	Glu dehydrogenase 2	Rice	1E-160
TC132821	1	gi|57899533	Plastidic Cys synthase 1	Rice	7E-126
TC146732	1	gi|469148	Ala aminotransferase	Barley	4E-81
TC134795	1	gi|108708268	Branched-chain amino acid aminotransferase	Rice	4E-48
Carbohydrate metabolism					
TC133521	3	gi|108864437	Glycosyl hydrolases family 38 protein, expressed	Rice	0
TC133163	3	gi|37535638	α-Galactosidase	Rice	0
TC133155	9	gi|50899994	β-Glucan-binding protein	Rice	0
TC132929	5	gi|18025340	α-L-Arabinofuranosidase/β-D-xylosidase	Barley	0

(*Table continues on following page.*)

Table II. (*Continued from previous page.*)

TIGR Accession	No. of Peptides Defining Group	NCBInr	Annotation	Organism	E Value
TC132139	3	gi|13398414	Arabinoxylan arabinofuranohydrolase	Barley	0
TC131885	3	gi|37535646	α-Galactosidase preproprotein	Rice	0
TC150244	1	gi|50510227	4-α-Glucanotransferase	Rice	0
TC133712	1	gi|50510292	α-Glucosidase II	Rice	0
TC149802	5	gi|1352328	Endo-1,3-β-glucosidase	Barley	9E-174
TC131099	1	gi|295806	(1-3,1-4)-β-D-Glucanase	Barley	1E-168
TC135072	1	gi|73622088	Xylanase inhibitor protein 1	Wheat	2E-164
TC130915	**4**	**gi|3037080**	**Glucan endo-1,3-β-glucosidase isoenzyme I**	**Barley**	**2E-160**
TC130923	1	gi|18865	Glucan endo-1,3-β-glucosidase	Barley	1E-155
TC143154	1	gi|50934913	GlcNAc-P mutase	Rice	4E-149
TC140649	1	gi|55168332	β-*N*-acetylhexosaminidase	Rice	2E-105
TC147598	4	gi|20160766	Xylanase inhibitor	Rice	3E-50
BG300456	1	gi|50938049	β-1,3-Glucanase	Rice	4E-48
BF627009	1	gi|55168332	β-*N*-acetylhexosaminidase	Rice	3E-38
Energy					
TC139468	3	gi|2493132	ATP synthase B-subunit isoform 2	Barley	0
TC139247	8	gi|11527563	Vacuolar proton-ATPase	Barley	0
TC130729	**4**	**gi|525291**	**ATP synthase β-subunit**	**Wheat**	**0**
TC132069	1	gi|50932993	Vacuolar ATP synthase subunit C	Rice	2E-175
Cytoskeleton					
TC146478	5	gi|4165488	α-Tubulin 3	Barley	0
TC132044	4	gi|77548264	Clathrin heavy chain	Rice	0
TC131561	5	gi|1743277	β-Tubulin 1	Barley	0
TC133559	1	gi|6094430	Tubulin α-2 chain	*Eleusine indica*	6E-94
TC146790	3	gi|1229169	Profilin	Barley	2E-61
Oxidative balance					
TC140370	3	gi|2759999	Peroxidase	Barley	0
TC148287	6	gi|50940483	Oxidase like	Rice	5E-174
TC131790	1	gi|57635161	Peroxidase 8	*T. monococcum*	8E-171
TC139150	8	gi|57635151	Peroxidase 3	*T. monococcum*	3E-149
TC147991	5	gi|108707054	NADH-dependent oxidoreductase 1	Rice	1E-148
TC148196	4	gi|57635165	Peroxidase 10	*T. monococcum*	3E-135
TC139337	1	gi|37530466	Peroxidase	Rice	1E-129
TC139146	1	gi|55700995	TPA: class III peroxidase 64 precursor	Rice	1E-104
TC151783	1	gi|55701007	TPA: class III peroxidase 70 precursor	Rice	6E-78
TC146841	4	gi|34911078	Peroxiredoxin	Rice	6E-77
TC146754	4	gi|6018682	Superoxide dismutase-4AP	*Z. mays*	1E-73
TC146479	5	gi|32186040	Thioredoxin h isoform 1; HvTrxh1	Barley	8E-62
TC146902	1	gi|32401362	Glutaredoxin	Wheat	2E-45
Defense					
TC139711	3	gi|50938485	Insulin-degrading enzyme	Rice	0
TC139653	3	gi|50916138	Oligopeptidase A like	Rice	0
TC132290	4	gi|50945443	Puromycin-sensitive aminopeptidase	Rice	0
TC131055	4	gi|6682829	Cys protease	*Z. mays*	0
TC147009	3	gi|18146827	Chitinase 2	Wheat	3E-153
TC148826	1	gi|34913680	DNA-damage-repair/toleration protein DRT102	Rice	3E-123
TC147216	1	gi|90959771	Multidomain cystatin	Rice	2E-114
TC150881	3	gi|50915254	Subtilisin-like proteinase	Rice	4E-98
TC139537	1	gi|3550467	cp31AHv protein	Barley	2E-95
TC139845	3	gi|62733218	Chitinase III C10701	Rice	1E-94
TC131676	**1**	**gi|1572627**	**Copper/Zn superoxide dismutase**	**Wheat**	**2E-78**
TC143082	1	gi|34910862	Pathogenesis-related protein	Rice	2E-72
TC140501	1	gi|62861391	Cold acclimation-induced protein 2-1	Wheat	1E-57
TC147802	1	gi|1617121	Subtilisin-chymotrypsin inhibitor 2	Barley	5E-32
Protein translation					
TC146747	12	gi|37534770	Endoplasmic reticulum membrane fusion protein	Rice	0
TC140222	3	gi|50948039	Glycyl-tRNA synthetase	Rice	0
TC146725	1	gi|77556802	60S ribosomal protein l2	Rice	3E-143
TC138849	5	gi|50940807	60S acidic ribosomal protein P0	Rice	1E-134
TC130710	3	gi|50252099	Ribosomal protein S4	Rice	2E-127

(*Table continues on following page.*)

Table II. (*Continued from previous page.*)

TIGR Accession	No. of Peptides Defining Group	NCBInr	Annotation	Organism	E Value
TC138786	1	gi|108862547	40S ribosomal protein S3a, expressed	Rice	1E-119
TC130754	1	gi|50939279	40S ribosomal protein	Rice	2E-119
TC131114	1	gi|57471706	Ribosomal protein L13a	Wheat	2E-105
TC146724	1	gi|77551804	40S ribosomal protein S9	Rice	7E-96
TC139071	1	gi|34893994	40S ribosomal protein S5	Rice	4E-95
TC139174	3	gi|50911805	60S ribosomal protein L12	Rice	2E-81
TC146756	1	gi|50934241	Ribosomal protein S12	Rice	3E-65
CV061576	1	gi|56783875	Acidic ribosomal protein P3a	Rice	1E-23
Protein folding					
TC147982	3	gi|34895466	66-kD stress protein	Rice	0
TC147147	6	gi|4056568	Protein disulfide isomerase-like protein	*Z. mays*	0
TC147130	5	gi|476003	Heat shock protein 70	Barley	0
TC146888	10	gi|34906196	Heat shock protein	Rice	0
TC146674	7	gi|1709617	Protein disulfide-isomerase precursor	Barley	0
TC138926	10	gi|50919489	Heat shock protein cognate 70	Rice	0
TC131381	9	gi|32765549	Heat shock protein 90	Barley	0
TC131558	**3**	**gi|92870233**	**Heat shock protein Hsp70**	***M. truncatula***	**0**
TC139542	2	gi|50919217	TCP-1/cpn60 chaperonin family protein	Rice	0
TC139525	1	gi|3023751	70-kD peptidyl-prolyl isomerase	Wheat	0
TC139412	1	gi|50913271	dnaK-type molecular chaperone precursor	Rice	0
TC146605	4	gi|13925734|	Cyclophilin A-2	Wheat	1E-88
Protein degradation					
TC148201	3	gi|50942477	Proteasome 26S non-ATPase subunit 1	Rice	0
TC131750	12	gi|401237	Ubiquitin-activating enzyme E1 2	Wheat	0
TC131582	3	gi|40643250	Cathepsin B	Barley	0
TC147593	1	gi|53792862	Proteasome activator subunit 4 like	Rice	0
TC134348	1	gi|50905317	26S proteasome regulatory subunit S2	Rice	0
TC132495	3	gi|50905317	26S proteasome regulatory subunit S2	Rice	8E-166
TC146450	3	gi|52548240	20S proteasome β 5 subunit	Wheat	3E-143
TC146981	5	gi|11967891	20S proteasome α-subunit	*Z. mays*	7E-130
TC131955	1	gi|66271075	β1 Proteasome-7D	*Aegilops tauschii*	6E-125
TC132063	4	gi|1709758	Proteasome α-subunit type 1	Rice	6E-124
TC139363	2	gi50931867	Proteasome α-subunit type 3	Rice	6E-124
TC132038	4	gi|17380182	Proteasome β-subunit type 1	Rice	2E-118
TC148954	1	gi|50918591	Sec63 domain-containing protein	Rice	8E-71
TC130753	6	gi|167073	Ubiquitin	Barley	3E-63
Signaling					
TC146926	10	gi|2499708	Phospholipase D α1	*Z. mays*	0
TC138584	14	gi|50909007	Elongation factor 2	Rice	0
TC132548	6	gi|50909927	Glycosylphosphatidylinositol-anchored protein	Rice	0
TC131653	3	gi|62997485	Protein phosphatase 2A regulatory a-subunit	*Z. mays*	0
TC130804	5	gi|53792733	Eukaryotic initiation factor 4A	Rice	0
TC149773	1	gi|3023693	Elongation factor 1-α	*Aureobasidium pullulans*	0
TC147364	1	gi|50919526	Phospholipase	Rice	0
TC146917	1	gi|50909061	RNA-binding protein Rp120	Rice	0
TC140422	1	gi|52353695	*N*-ethylmaleimide sensitive fusion protein	Rice	0
TC139879	1	gi|50920113	Translational elongation factor Tu	Rice	0
TC139323	1	gi|1737492	Poly(A)-binding protein	Wheat	0
TC146710	4	gi|50906401	Elongation factor 1-γ	Rice	1E-178
TC140179	2	gi|33146739	GPI-anchored protein like	Rice	2E-158
TC139070	5	gi|22607	14-3-3 Protein homolog	Barley	3E-142
TC139287	1	gi|51535961	Protein phosphatase 2C	Rice	2E-140
TC139604	3	gi|50920031	Late embryogenesis abundant protein	Rice	2E-135
TC140571	5	gi|20804751	Cytosolic factor-like protein	Rice	4E-122
TC146854	3	gi|52346236	Acid phosphatase	Barley	4E-121
TC131959	3	gi|108711028	Stem-specific protein TSJT1	Rice	1E-108
TC139972	1	gi|108707683	Pathogenesis-related protein 1	Rice	5E-78
TC138855	**3**	**gi|232033**	**Elongation factor 1-β**	**Wheat**	**7E-70**
TC146685	1	gi|728594	Gly-rich protein, RNA-binding protein	Barley	5E-42
TC147175	6	gi|54778542	Horcolin	Barley	3E-31

(*Table continues on following page.*)

Table II. (*Continued from previous page.*)

TIGR Accession	No. of Peptides Defining Group	NCBInr	Annotation	Organism	E Value
Transport					
TC152581	3	gi|29123368	High-affinity phosphate transporter	Barley	0
TC147625	3	gi|50934997	Coatomer protein γ 2-subunit	Rice	0
TC146833	3	gi|53982658	GDP dissociation inhibitor	Rice	0
TC139045	4	gi50400847	H+-ATPase	Wheat	0
TC131757	2	gi|62900380	Importin α-1b-subunit	Rice	0
TC146836	1	gi|6691629	HvPIP1;3	Barley	2E-151
TC148527	1	gi|23954314	Transportin	Rice	4E-123
BJ464951	1	gi|7339699	Importin-α reexporter	Rice	3E-90
Unknown					
TC134738	6	gi|18146791	D protein	Barley	0
TC130945	6	gi|4158232	Reversibly glycosylated polypeptide	Wheat	0
TC148380	1	gi|52077208	Unknown protein	Rice	0
TC147606	1	gi|19071	Protein zx	Barley	0
TC146779	1	gi|50921575	OSJNBa0027H09.17	Rice	0
TC146718	1	gi|1408512	|dbj|BAA13068.1|	Rice	0
TC139280	1	gi|2072727	Fd-GOGAT protein	Rice	0
TC138693	1	gi|50926280	OSJNBa0014K14.18	Rice	0
TC131623	1	gi|50931573	|ref|XP_475314.1|	Rice	0
TC131033	1	gi|31296711	GAD1	Barley	0
TC139573	1	gi|37535140	|ref|NP_921872.1|	Rice	6E-178
TC130742	4	gi|108707930	Expressed protein	Rice	8E-177
TC131324	3	gi|50923165	OSJNBa0008A08.11	Rice	1E-174
TC133361	1	gi|57899406	Helicase-B-associated transcript 1	Rice	4E-161
TC131647	1	gi|46805936	|dbj|BAD17230.1|	Rice	2E-160
TC140535	2	gi|50929321	OSJNBa0011F23.4	Rice	3E-159
TC147335	1	gi|51963828	P0575F10.14	Rice	1E-158
TC132188	5	gi|50923829	OSJNBa0044M19.9	Rice	1E-154
TC139943	1	gi|50915982	KH domain-containing protein NOVA like	Rice	6E-148
TC147431	1	gi|54291831	Unknown protein	Rice	4E-140
TC131062	1	gi|50948271	|ref|XP_483663.1|	Rice	3E-118
TC132224	4	gi|50915640	SPATULA like	Rice	4E-111
TC147192	1	gi|50923623	OSJNBa0069D17.2	Rice	2E-107
TC140155	1	gi|50511386	Unknown protein	Rice	4E-106
AV835541	1	gi|50938581	Karyopherin-β 3 variant	Rice	2E-98
TC147995	1	gi|77552020	Patatin-like protein	Rice	3E-96
TC131723	1	gi|3702665	|emb|CAA07474.1|	Rice	5E-87
TC135855	2	gi|50932957	Unknown protein	Rice	3E-82
TC142088	1	gi|37537066	Unknown protein	Rice	3E-81
TC136407	1	gi|6815075	MAWD-binding protein	Rice	8E-80
TC147301	1	gi|55700995	|tpe|CAH69306.1|	Rice	1E-73
TC132108	1	gi|50939495	|ref|XP_479275.1|	Rice	2E-73
TC153068	1	gi|27261082	Unknown protein	Rice	3E-70
TC139514	1	gi|32492140	|emb|CAE03373.1|	Rice	5E-68
TC147815	1	gi|34908928	Latex-abundant protein	Rice	4E-66
TC136015	1	gi|50911579	GAMM1 protein	Rice	4E-66
TC131126	1	gi|21322752	|dbj|BAB78536.2|	Rice	7E-62
TC141421	1	gi|34910236	Unknown protein	Rice	6E-54
TC131726	1	gi|34899866	Unknown protein	Rice	1E-48
TC141742	1	gi|51091938	PrMC3	Rice	3E-46
BQ768779	1	gi|52353425	Unknown protein	Rice	6E-44
TC136111	1	gi|50926656	OSJNBa0074L08.23	Rice	2E-41
BQ763407	1	gi|50252172	Senescence-associated protein like	Rice	4E-36
AL511164	1	gi|90399278	H0306F03.6	Rice	2E-33
TC147252	1	gi|50915240	|ref|XP_468084.1|	Rice	1E-28
TC134176	1	gi|83647364	FAD/FMN-containing dehydrogenase	*Hahella chejuensis*	1E-26
TC131063	1	gi|50904847	Gly-rich protein 2	Rice	1E-26
TC145521	1	gi|50929757	OSJNBa0088H09.2	Rice	9E-26
TC146830	1	gi|50919281	|ref|XP_470037.1|	Rice	2E-25

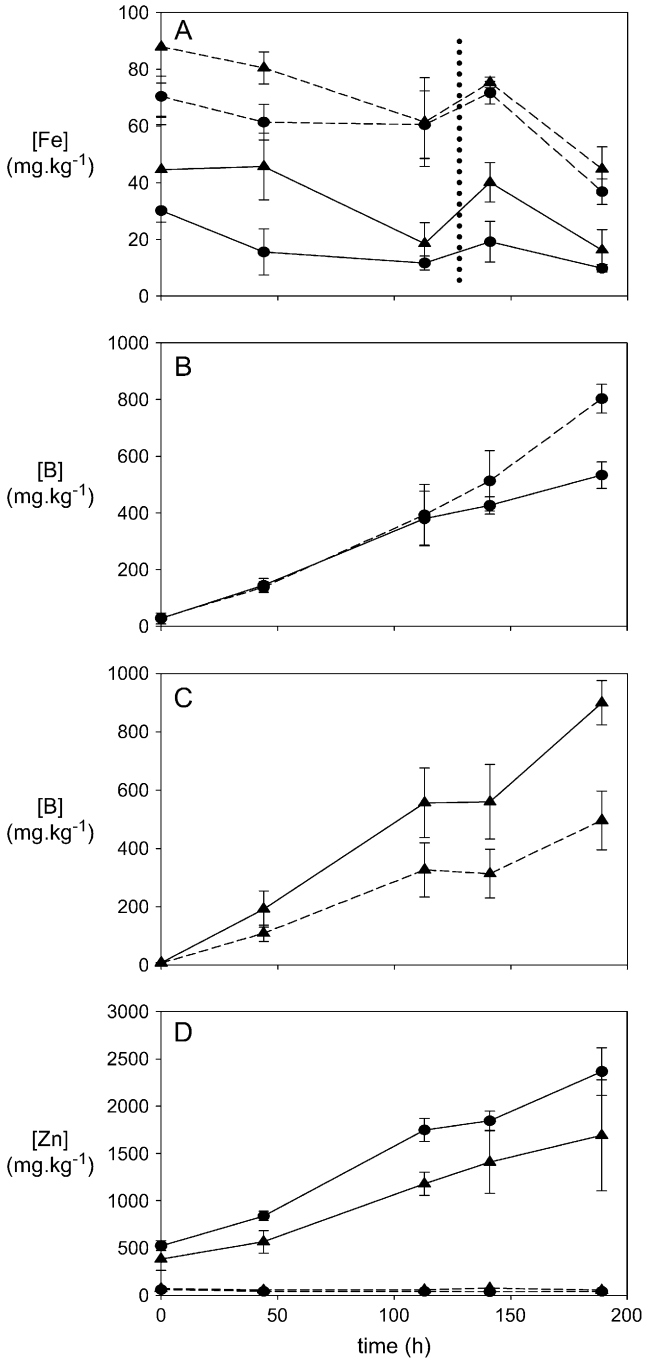

Figure 5. Inductively coupled plasma analysis of elemental abundance in barley leaves from B-tolerant ('Sahara') and B-intolerant ('Clipper') plants. A, Fe concentrations in the youngest leaves. B, Accumulation of B in the oldest leaf of 'Clipper.' C, Accumulation of B in the oldest leaf of 'Sahara' plants. D, Zn accumulation in oldest leaves. Circles, 'Clipper' plants; triangles, 'Sahara.' Dashed lines, Fe-replete plants; solid lines, Fe-deficient plants. Dotted vertical line in A indicates emergence of fourth (new) leaf. Error bars indicate SD ($n = 3$).

The iTRAQ approach used in this study represents a robust and accurate method of comparing protein abundances between proteins isolated from plants of differing genotypes or variable treatments. This method compares favorably with other proteomic approaches, notably two-dimensional (2D)-PAGE, particularly in relation to the quantitative aspect of the iTRAQ analysis. In terms of the functions of the proteins identified in this study, strong similarities exist in data sets from other cereals, namely wheat (*Triticum aestivum*) and rice (*Oryza sativa*; Koller et al., 2002; Donnelly et al., 2005; Nozu et al., 2006). Enzymes involved in biosynthetic metabolic pathways dominated the identifications, while 10 distinct components of the proteasome were also identified in the root protein complement.

In monocotyledonous crop species, proteomic studies have focused on rice for a range of reasons, one of which is the availability of a complete genome

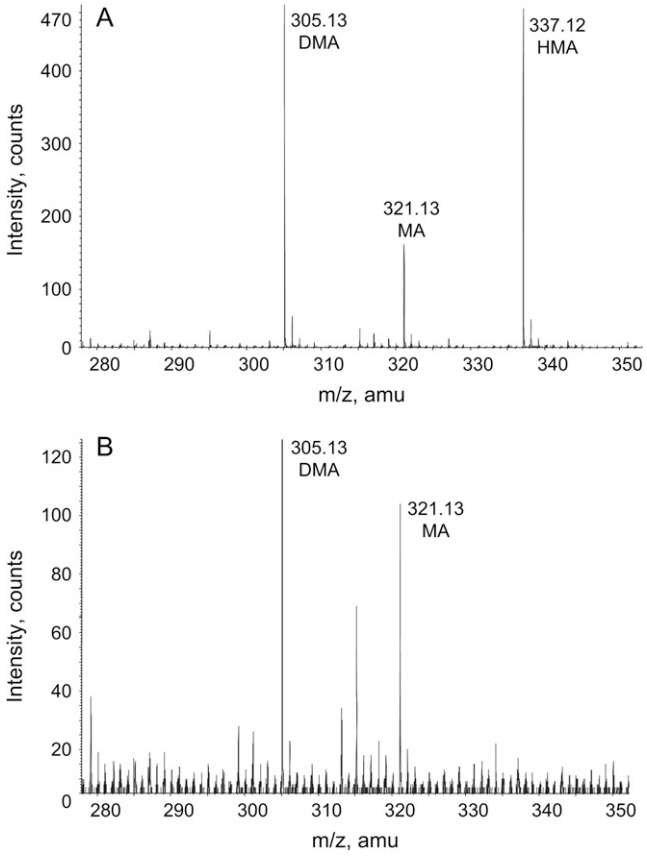

Figure 6. MS analysis of siderophores collected from the root secretions of 'Sahara' and 'Clipper' plants. 'Sahara' (A) and 'Clipper' (B) plants were grown in Fe-deficient conditions. Secretions were collected after 10 d of growth in Fe-deficient conditions. All siderophores were identified as singly charged species in the positive ion mode. Samples were purified by fractionation using cation-exchange resin, dried, and resuspended in methanol/1% formic acid (v/v) and infused directly into the MS. We cannot discount the possibility of other coextracted compounds potentially suppressing the siderophore signals in either sample. As such, relative signal intensities between extracts were not considered.

sequence (Goff et al., 2002; Rossignol et al., 2006). The ever-increasing size of EST and genomic sequence databases for other cereal species is rapidly creating a situation where proteomic analyses in other graminaceous crop plants are feasible. In this study, we searched MS/MS spectra exclusively against the EST assemblies in the TIGR barley gene index (V9.0). Of the 479 barley proteins matched against this database, only 86 (18%) matched barley proteins in the National Center for Biotechnology Information (NCBI) NCBInr protein database. Sixty percent of the 479 proteins matched to rice orthologs in the NCBInr protein database, highlighting the usefulness of EST-derived databases for proteomic studies (Tables I and II) in cereals that lack a completely sequenced genome.

Notably, there were fewer large differences (>2.5-fold) between peptides identified in the bulked segregant analysis (1.05%) compared to the analysis of peptides from the leaves of 'Golden Promise' plants (3.96%). This was despite a fractionally larger spread across the majority of iTRAQ ratios in the bulked segregant analysis, as evidenced by comparison of the width of boxes and error bars in Figures 2A and 4A. It appears that using a bulked segregant approach, in combination with a proteomic comparison, may represent a fruitful avenue to investigate the nature of novel QTL in barley as well as other cereals.

Previous studies comparing the protein profiles of root and leaf tissues have identified variable overlaps in the percentages of shared proteins. In a recent 2D-PAGE analysis of rice tissues, Nozu et al. (2006) identified similar numbers of protein identifications to that described in this study but found a 22% overlap in the identity of proteins found in root and leaf tissue. An earlier study, while identifying more proteins using a combination of 2D-PAGE and MudPIT approaches, found a 5% match between root and leaf proteins (Koller et al., 2002). The 2% overlap in protein expression described in this study is in approximate agreement with the latter study.

Contrasting with this relatively low overlap at the level of protein abundance, metabolite profiles of different tissues have a much higher degree of similarity (Roessner et al., 2006). Disregarding the small differences in metabolite abundances between varieties, comparison of the metabolite profiles of both 'Clipper' and 'Sahara' root and leaf tissues shows a high degree of overlap. Of the 68 metabolites identified and measured in roots of each cultivar, 63 were also present in leaves, representing an over 90% overlap in metabolite production between tissues (Roessner et al., 2006). This comparison reinforces the notion of tissue-specific expression of enzymes responsible for production of the same metabolite.

It is of note that a recently described tissue-specific barley transcript database reports over 12,000 expressed genes in both root and leaf tissues (Druka et al., 2006). It would be interesting to correlate the overlap in transcript and protein levels between these two tissues, particularly given the potential of this type of analysis to provide insights into posttranslational regulation of protein expression.

Proteins Involved in Siderophore Production Pathway Elevated in B-Tolerant Plants

Along with the identification of elevated levels of IDS2 and IDS3, we also identified a number of enzymes mediating upstream steps in the Yang cycle (Negishi et al., 2002). This pathway produces nicotianamine, the precursor of HMA. Levels of MTK were also elevated in the tolerant plants. Other proteins involved in the Yang cycle, namely METS1, IDI2, adenosyl phoshoribosyl transferase, and SAM sythetase did not notably differ in abundance between tolerant and intolerant plants. METS is notable because of the large number of identified peptides matching to this protein (Table II), indicating that this protein may be relatively abundant in the roots of barley plants. This is despite the product of this enzyme, Met, occurring at relatively low steady-state levels in the roots of barley plants (Ma et al., 1995).

A recent gas chromatography-MS-based analysis compared the abundances of metabolites isolated from the roots and leaves of 'Clipper' and 'Sahara' (Roessner et al., 2006). The precursor metabolites for siderophore production that were measured in this study, Met and Asp, as well as γ-aminobutyrate, were found to be present in comparable amounts in both the roots and leaves of each genotype. Despite these steady-state similarities, however, it is quite possible that the fluxes of metabolites passing through these pathways may differ significantly between cultivars. It may also be interesting to examine the levels of SAM and nicotiamine in the two cultivars, as these metabolites are the immediate precursors for siderophore production.

The chromosomal locations of *ids2* and *ids3* genes have been identified; *ids2* maps to the long arm of chromosome 7H, while *ids3* maps to the long arm of chromosome 4H (Nakanishi et al., 2000). Both appear to be single copy genes (Nakanishi et al., 2000). The chromosomal locations of genes encoding MTK and the D protein are currently unknown. Nonetheless, it is more probable that the genetic difference underpinning the elevated abundance of these proteins is a regulatory factor that coordinately controls the abundances of these proteins, perhaps functioning as a transcription factor. It is noteworthy that the transcripts of the significantly elevated proteins in this study have all previously been identified as being Fe inducible in barley roots (Negishi et al., 2002 and refs. therein). The genes encoding these proteins all share the same Fe Deficiency Response Element1 (IDE1)-like upstream elements (Kobayashi et al., 2003, 2005). Any candidate transcription factor may share some similarities to the recently identified IDE1-recognizing, Fe-regulated transcription factor IRO2 (Ogo et al., 2006). Significantly, however, IDE1-type sequences are also present upstream of proteins that were not elevated in

the B-tolerant plants, specifically SAM sythetase and IDI2.

Plant Fe Status and B Uptake

To begin to differentiate if the increased abundance of siderophore-producing enzymes in the B-tolerant plants was merely associated with the B tolerance loci rather than being responsible for the tolerance trait per se, we examined the effects of Fe availability on B uptake. Fe-deficient 'Sahara' plants accumulated more B than the Fe-replete plants, highlighting a potential breakdown of the B-tolerance mechanism in this situation. The effect was observed immediately upon removal of Fe from the growing medium. In contrast, Fe deficiency had no effect on the rate of B accumulation in 'Clipper' plants initially, although over time (>110 h), the rate of B accumulation decreased. This situation is reminiscent of studies showing similar increases in B accumulation during Zn deficiency in barley (Graham et al., 1987).

The increased rate of leaf Zn accumulation supported the notion that Fe deficiency resulted in an increase in siderophore production, supporting the recent demonstration of the involvement of MA-related compounds in the uptake of Zn (von Wiren et al., 1996; Suzuki et al., 2006). Notably, high B alone had no effect on leaf Zn levels (Fig. 5). Although graminaceous monocots primarily employ a siderophore-dependent Fe acquisition strategy (Mori, 1999), it is also possible that Fe deficiency results in increased uptake of Zn through nonspecific Fe(II) transporters, possibly similar to *Os*IRT1 (Bughio et al., 2002), which may be upregulated in Fe-deficient conditions.

Modeling an Interaction between HMA and B

The proteomics-based identification of elevated levels of IDS2 and IDS3 in the B-tolerant plants led us to consider any possible interactions between B, siderophores (particularly HMA or eHMA), and Fe. As an initial step, we used molecular modeling based on the available crystallographic data from a Cu(II) complex of MA (Nomoto et al., 1981) to determine the feasibility of any interaction between B, Fe, and HMA or eHMA. This analysis suggested that Fe(III) HMA, which has the carboxylate group and the hydroxyl group on the same side of the four-membered ring (a cis arrangement), is more likely to be able to bind a B center than the Fe(III) eHMA.

The recent identification of B complexation with vibrioferrin, a bacterial siderophore (Amin et al., 2007), provides support for the notion of B-siderophore interactions occurring in extracellular environments. A key difference between the B-vibrioferrin interaction and the B-HMA interaction proposed here, however, is the dependence upon complexed Fe(III) in the HMA model. In conditions where Fe is available, an Fe(III) HMA-B interaction may result in a decreased B influx, analogous to the mechanism of aluminum-malate chelation described in wheat (Delhaize et al., 1993). Localized, high concentrations of Fe(III) HMA adjacent to the site of B movement across the PM may be sufficient to partially decrease the rate of B accumulation in planta. Further work will be needed to test this proteomics-driven hypothesis, and we intend to explore this model in the future.

The enzyme responsible for the production of HMA, via the hydroxylation of MA at C3, has not yet been described. Although the hydroxylation reactions catalyzed by IDS2 (producing *e*HMA) and IDS3 are similar and each protein contains the requisite residues for Fe^{2+} and 2-oxoglutarate binding (Fig. 7), each protein catalyzes addition of hydroxyl groups to distinct carbon residues. Despite this catalytic selectivity, the two proteins are 55% identical at the amino acid level (Fig. 7). It is highly likely that IDS2 and the protein responsible for the production of HMA, tentatively named IDS2b, share an even greater level of amino acid identity. It is therefore feasible that the peptides identified

Figure 7. Sequence alignment of barley IDS2 (gi 285634) and IDS3 (gi 9711238) proteins, with peptides identified by MS/MS underlined. Identical residues are indicated by asterisks. Arrows indicate conserved residues required for Fe(II) and 2-oxoglutarate binding.

as matching to IDS2 may indeed be derived from regions of identity within the uncharacterized IDS2b protein.

CONCLUSION

We are currently working toward verifying any interaction between B, Fe, and HMA. We are also in the process of defining which tolerance locus (4H or 6H) may be responsible for this trait, although we believe it is more likely that HMA production may be linked to the weaker 6H tolerance locus. This postulate is based on the proposal of Hayes and Reid (2004) that the major tolerance locus may encode a protein responsible for B efflux. To this end, we intend to compare the PM protein profiles from the bulked segregants analyzed in this study using the iTRAQ approach we described.

In conclusion, we have described a robust and reliable new comparative proteomic methodology. This approach has wide-ranging applications, particularly in the field of cereal functional genomics. Protein abundance data collected using this method will be able to be interpreted in conjunction with the increasingly large metabolomic and transcriptomic data sets continuing to appear in the literature.

MATERIALS AND METHODS

All chemicals were purchased from Sigma-Aldrich unless otherwise specified.

Plant Growth

Barley (*Hordeum vulgare*) seeds ('Golden Promise,' 'Clipper,' and 'Sahara' and selected lines from the 'Clipper' × 'Sahara' DH population, selected as described in ''Results''; Jeffries et al., 1999) were surface sterilized with 70% (v/v) ethanol and 0.5% (v/v) sodium hypochlorite prior to imbibing for 16 h in distilled water with aeration. Seeds were then transferred to moist filter paper and grown until coleoptiles were approximately 30 mm in length. Seedlings were then suspended over 15 L of hydroponic growth solution (36 plants per container) composed of 5 mM NH_4NO_3, 5 mM KNO_3, 2 mM $Ca(NO_3)_2$, 2 mM $MgSO_4$, 0.1 mM KH_2PO_4, 0.5 mM Na_2SiO_3, 50 μM NaFe(III) EDTA, 5 μM $MnCl_2$, 10 μM $ZnSO_4$, 0.5 μM $CuSO_4$, 0.1 μM Na_2MoO_3, and 50 μM H_3BO_3. The solution was gently aerated and changed after 1 week initially and every 3 d subsequently. Plants were grown in a growth chamber using a 13°C, 10-h dark period and an 18°C, 14-h light period (180 μmol m^{-2} s^{-1} photon intensity).

For B tissue accumulation experiments, plants were grown as described, except for the Fe-deficient plants, which were grown in solutions lacking NaFe(III) EDTA. After seedling establishment for 1 week, all 'Clipper' plants were transferred to solutions containing 1 mM H_3BO_3, while 'Sahara' plants were transferred to solutions containing 5 mM H_3BO_3. Oldest and youngest leaves were harvested at indicated time points, dried, and elemental composition was determined using inductively coupled plasma optical emission spectrometry as described in Roessner et al. (2006). Earlier studies had determined that the rate of B accumulation in the oldest leaf in 'Clipper' plants grown in 1 mM B was similar to that of 'Sahara' plants grown in 5 mM B (Fig. 2 from Roessner et al., 2006). Using this information, the effect of Fe nutritional status on the rate of B accumulation in each cultivar was followed over similar time frames by growing each cultivar in different levels of B: 1 mM for 'Clipper' and 5 mM for 'Sahara' (Fig. 5). In the experiments described here, the rate of B accumulation in the 'Clipper' plants grown at 1 mM B was approximately double that of 'Sahara' plants grown in 5 mM B in Fe-replete conditions. Initial experiments also indicated that elevated levels of B (1 mM for 'Clipper,' and 5 mM for 'Sahara') had no effect on Fe accumulation in the youngest leaves of either cultivar (data not shown).

Protein Isolation

After 2 weeks of growth, roots and leaves were harvested 3 h after the beginning of the light period. Tissues were weighed and suspended in 2 volumes of chilled homogenization buffer containing 50 mM phosphate buffer, pH 7.5, 20 mM KCl, 0.5 M Suc, 10 mM dithiothreitol, 0.2 mM phenylmethylsulfonyl fluoride, 10 mM EDTA, and 10 mM EGTA. Tissues were homogenized with a curved, hand-held blade, filtered through a 50-μm nylon mesh, and centrifuged at 6,000*g* for 10 min. The supernatant from this step was centrifuged at 100,000*g* for 1 h. The final supernatant was concentrated by precipitation with two volumes of −20°C equilibrated 10% (w/v) TCA in acetone for 16 h at −20°C. The resulting pellet was washed twice with −20°C equilibrated 90% (v/v) acetone before resuspension in 0.5 M triethylammonium bicarbonate, pH 8.5, containing 0.1% SDS. The protein concentration was determined at this stage using a 2D Quant kit (GE Healthcare).

Protein Digestion and iTRAQ Labeling

Protein (100 μg) was reduced by addition of 5 mM tris-(2-carboxyethyl) phosphine and incubation at 60°C for 1 h. Cys residues were then blocked by incubation with 90 mM methyl methanethiosulfonate (MMTS) for 10 min at room temperature. $CaCl_2$ (1 mM) was then added, and proteins were digested with modified trypsin (4 μg, sequencing grade, porcine, Promega) for 16 h at room temperature in a final volume of 40 μL. iTRAQ tags (Applied Biosystems) were resuspended in ethanol, and digestion was stopped by addition of iTRAQ tag/ethanol solution to a final concentration of 70% (v/v) ethanol. iTRAQ labeling was allowed to proceed for 1 h at room temperature. Labeled peptide mixtures were then pooled for chromatography.

Peptide Chromatography

iTRAQ-labeled peptide mixtures were dried under a stream of N_2 and resuspended in 100 μL of 25 mM ammonium formate, pH 3.5, containing 5% acetonitrile (buffer A). Peptides were fractionated as described in Wagner et al. (2003) with some modifications. Samples were injected onto a strong-cation exchange (SCX) column (polysulfoethyl A 200 × 4.6 mm, 5 μM, 300 Å) using an Agilent HPLC with an automatic fraction collector. Peptides were eluted with a gradient from 100% buffer A to 100% 0.5 M ammonium formate, pH 3.5, containing 25% acetonitrile over 30 min with a flow rate of 0.7 mL min^{-1}. Generally, 60 fractions (350 μL each) were collected. These fractions were dried under vacuum and stored at −20°C.

Individual SCX fractions were resuspended in 0.1% formic acid (60 μL) and loaded onto a 300-μm × 5-mm C18 precolumn. After washing the precolumn with 0.1% formic acid, peptides were eluted from the precolumn onto an in-line C18 column (75 μm i.d. × 15 cm, 3 μm/100 Å Vydac) and fractionated using a gradient of 0% to 70% (v/v) acetonitrile in 0.1% formic acid over 60 min, using a flow rate of 0.25 μL min^{-1}. This column eluted directly into a QSTAR XL hybrid quadropole-time of flight instrument (Applied Biosystems/MDS Sciex) using a nanospray source.

MS

The mass spectrometer was operated in the positive ion mode, ion source voltage of 1,750 V, using 10-μm uncoated SilicaTips (New Objectives). Data were collected using AnalystQS software in a data-dependent acquisition mode for the three most intense ions fulfilling the following criteria: m/z between 450 and 2,000; ion intensity >40 counts; and charge state between 2^+ and 4^+. After MS/MS analysis, these ions were dynamically excluded for 20 s, using a mass tolerance of 250 ppm. MS scans were accumulated for 0.5 s, and MS/MS scans were accumulated for 2 s. A mass and charge state-dependent rolling collision energy was used and was 20% to 30% greater than was used for an iTRAQ-unlabeled peptide. The MS was calibrated daily with [Glu]-fibrinopeptide B.

MS/MS Spectra Interrogation

Peak lists from individual data files were created using the MASCOT.dll script in AnalystQS 1.1 and interrogated using MASCOT (Matrix Science, Perkins et al., 1999) and X!Tandem (Robertson and Beavis, 2004). In both cases, the spectra were searched against a six-frame translation of the Barley V9.0 Gene Index (TIGR, released September 15, 2004). MASCOT parameters were as follows: MS peptide tolerance ±0.25 D, MS/MS tolerance ±0.15 D, trypsin

cleavage, allowing one missed cleavage, fixed modifications of iTRAQ tags on N terminus, and Lys residues and MMTS and variable modification of iTRAQ on Tyr residues. The X!Tandem parameters were fragment mass error 0.2 D, parent mass tolerance ±100 ppm, minimum peak 15, maximum peak of 500, complete modification of N terminus with iTRAQ and MMTS on Cys, and potential modifications were iTRAQ on Lys and Tyr, with a maximum of one missed cleavage.

We used an in-house Linux script that collated the MASCOT, X!Tandem, and i-Tracker outputs (see below) from all data files representing an entire series of SCX fractions into a single file. Peptides were only reported if they had a MASCOT score greater than 37 ($P < 0.05$). Peptides that lacked a C-terminal Lys or Arg residue were rejected. The X!Tandem output was formatted into a single column, showing whether the MASCOT-identified peptide was identified by X!Tandem. When multiple spectra from the SCX dataset were matched to the same peptide, only the match with the highest MASCOT score was reported.

Based on preliminary work comparing MS/MS search algorithm outputs against manually checked MS/MS spectra ($n = 400$), we found that automatic acceptance of protein matches based on one peptide can result in a high proportion of false positives. As such, we adopted a conservative approach to protein identification in this study. Accessions were accepted using a two-tiered criteria. If three or more peptides (identified solely by MASCOT, score >37) matched to a single accession, the identification was automatically accepted. Using a three-peptide-matches criteria, reverse database searching gave a false positive rate of <1%. Accessions containing one or two peptides were then accepted if at least one peptide was also matched using X!Tandem (peptide accepted by two independently developed algorithms). Only peptides matched by the two algorithms were reported.

Peptide Grouping

Accessions were manually grouped into protein families, or groups of accessions that shared peptides. All peptides within a protein family are unique to that family. This feature of multiple accessions matching to groups of peptides is exacerbated in cereal genomes, where polyploidy results in large families of genes with very similar sequences.

To generate protein identifications from the accession matches, the nucleotide sequence of each matched accession was searched against the NCBInr protein database (BLASTX), using the default parameters. BLAST searches were performed between April and August, 2006.

iTRAQ Ratio Determinations

The tagged peptides were then pooled and fractionated using a SCX column, followed by C_{18} reversed-phase HPLC, directly interfaced via an ESI source to the MS. Due to the identical chemical nature of the iTRAQ tags, identical peptides from the differentially labeled samples cofractionate and enter the MS and are analyzed simultaneously. During MS/MS analysis of peptides, the reporter ions, derived from the isotopically distinct iTRAQ tags, are released from the differentially tagged peptides. The relative abundance of the reporter ions is representative of the relative abundance of the peptides in the starting mixtures.

iTRAQ tags attach to secondary amine groups, such that in the case of trypsin-derived peptides, tags are attached to both N- and C-terminal ends of each peptide. This increases the amount of energy required to fragment the peptide to generate amino acid information but also improves the quality of the MS/MS spectra, such that more y- and b-ions are observed (Fig. 1B).

iTRAQ ratios were generated using the open source software i-Tracker (Shadforth et al., 2005). We used a reporter ion peak intensity threshold of 10, rejecting ratios with an associated error of greater than 4. We also rejected ratios derived from reporter ions which, after summing the relative peak areas for the tags employed in that experiment, contributed to less than 80% to the total area of all four reporter ion peaks (m/z 114–m/z 117). Ratios were then normalized around 1 by multiplication of all ratios by the average value of the ratios. Normalized ratios were finally log transformed to generate a normally distributed set of data.

Siderophore Purification and Analysis

Siderophores were collected as described by Takagi et al. (1984). Plants were removed from the hydroponic growing solution, and roots were placed in gently aerated distilled water. Root secretions were collected over 3 h. This solution was concentrated 10-fold using rotary evaporation. The concentrated root secretions were fractionated on an Amberlite IR120 cation exchange resin, washed with water, and siderophores were then eluted from the resin with 1 M NH_4OH. The eluate was dried under vacuum and resuspended in 50% methanol and 0.1% formic acid. ESI-MS analysis was performed in the positive ion mode, with samples directly infused into the QSTAR XL hybrid quadropole-time of flight instrument. The MS/MS fragmentation profile of the siderophores shared features with the collision-induced dissociation profiles of MA described by Kenny and Nomato (1994; data not shown).

Supplemental Data

The following materials are available in the online version of this article.

Supplemental Figure S1. Number of peptides that match to distinct proteins.

Supplemental Figure S2. Plot of relative peak areas of reporter ions 115 and 114 from 480 peptides with iTRAQ ratios from 'Golden Promise' leaves.

Supplemental Figure S3. Plot of relative peak areas of reporter ions 115 and 114 from the 1,038 peptides with iTRAQ ratios from B-tolerant and B-intolerant barley roots.

Supplemental Table S1. Complete list of peptides identified from barley 'Golden Promise' leaf tissue.

Supplemental Table S2. Complete list of peptides identified from barley root tissue (B-tolerant and B-intolerant 'Clipper' × 'Sahara' DH lines).

ACKNOWLEDGMENTS

We thank Ed Newbigin, Brendan Abrahams, Tim Sutton, Andreas Schreiber, Mark Tester, Ute Baumann, and Margie Pallotta for helpful suggestions and discussions.

Received January 22, 2007; accepted April 30, 2007; published May 3, 2007.

LITERATURE CITED

Amin SA, Kupper FC, Green DH, Harris WR, Carrano CJ (2007) Boron binding by a siderophore isolated from a marine bacteria associated with the toxic dinoflagellate *Gymnodium catenatum*. J Am Chem Soc **129:** 478–479

Bughio N, Yamaguchi H, Nishizawa NK, Nakanishi H, Mori S (2002) Cloning an iron-regulated metal transporter from rice. J Exp Bot **53:** 1677–1682

Cartwright B, Zarcinas BA, Mayfield AH (1984) Toxic concentrations of boron in a red-brown earth at Gladstone, South Australia. Aust J Soil Res **22:** 261–272

Delhaize E, Ryan PR, Randall PJ (1993) Aluminum tolerance in wheat (Triticum aestivum L.). II. Aluminum-stimulated excretion of malic acid from root apices. Plant Physiol **103:** 695–702

Donnelly BE, Madden RD, Ayoubi P, Porter DR, Dillwith JW (2005) The wheat (Triticum aestivum L.) leaf proteome. Proteomics **5:** 1624–1633

Druka A, Muehlbauer G, Druke I, Caldo R, Baumann U, Rostoks N, Schreiber A, Wise R, Close T, Kleinhofs A, et al (2006) An atlas of gene expression from seed to seed through barley development. Funct Integr Genomics **6:** 202–211

Goff SA, Ricke D, Lan T, Presting G, Wang R, Dunn M, Glazebrook J, Sessions A, Oeller P, Varma H, et al (2002) A draft sequence of the rice genome (*Oryza sativa* L. ssp. *japonica*). Science **296:** 92–100

Graham RD, Welch RM, Grunes DL, Cary EE, Norvell WA (1987) Effect of zinc deficiency on the accumulation of boron and other mineral nutrients in barley. Soil Sci Soc Am J **51:** 652–657

Hayes JE, Reid RJ (2004) Boron tolerance in barley is mediated by efflux of boron from the roots. Plant Physiol **136:** 3376–3382

Jeffries SP (2000) Marker assisted backcrossing for gene introgression in barley (*Hordeum vulgare* L.). PhD thesis. Department of Plant Science, University of Adelaide, Australia

Jeffries SP, Barr AR, Karakousis A, Kretschmer JM, Manning S, Chalmers KJ, Nelson JC, Islam AKMR, Langridge P (1999) Mapping of chromosome regions conferring boron toxicity tolerance in barley (*Hordeum vulgare* L.). Theor Appl Genet **98:** 1293–1303

Karakousis A, Barr AR, Kretschmer JM, Manning S, Jeffries SP, Chalmers KJ, Islam AKM, Langridge P (2003) Mapping and QTL analysis of the barley population Clipper x Sahara. Aust J Agric Res **54:** 1137–1140

Kenny PTM, Nomato K (1994) Tandem mass spectrometric investigation of phytosiderophores mugineic acid, deoxymugineic acid and nicotianamine. Analyst **119:** 891–895

Kobayashi T, Nakayama Y, Itai RN, Nakanishi H, Yoshihara T, Mori S, Nishizawa NK (2003) Identification of novel *cis*-acting elements, IDE1 and IDE2, of the barley *IDS2* gene promoter conferring iron-deficiency-inducible, root-specific expression in heterogeneous tobacco plants. Plant J **36:** 780–793

Kobayashi T, Suzuki M, Inoue H, Itai R, Takahashi M, Nakanashi H, Mori S, Nishizawa NK (2005) Expression of iron acquisition-related genes in iron-deficient rice is co-ordinately induced by partially conserved iron-deficiency-responsive elements. J Exp Bot **56:** 1305–1316

Koller A, Washburn MP, Langer BM, Andon NL, Deciu C, Haynes PA, Hays L, Schiletz D, Ulaszek R, Wei J, et al (2002) Proteomic survey of metabolic pathways in rice. Proc Natl Acad Sci USA **99:** 11969–11974

Ma JF, Shinada T, Matsuda C, Nomoto K (1995) Biosynthesis of phytosiderophores, mugineic acids, associated with methionine cycling. J Biol Chem **270:** 16549–16554

Michelmore RW, Paran I, Kesseli RV (1991) Identification of markers linked to disease-resistance genes by bulked segregant analysis: a rapid method to detect markers in specific genomic regions by using segregating populations. Proc Natl Acad Sci USA **88:** 9828–9832

Mori S (1999) Iron acquisition by plants. Curr Opin Plant Biol **2:** 250–253

Mori S, Nishizawa N (1987) Methionine as a dominant precursor of phytosiderophores in *Graminaceae* plants. Plant Cell Physiol **28:** 1081–1092

Nable RO (1988) Resistance to boron toxicity amongst several barley and wheat cultivars: a preliminary examination of the resistance mechanism. Plant Soil **112:** 45–52

Nable RO, Cartwright B, Lance RC (1990) Genotypic differences in boron accumulation in barley: relative susceptibilities to boron deficiency and toxicity. *In* N El Bassam, M Dambroth, B Loughman, eds, Genetic Aspects of Plant Mineral Nutrition. Kluwer Academic Publishers, Dordrecht, The Netherlands, pp 243–251

Nakanishi H, Yamaguchi H, Sasakuma T, Nishizawa NK, Mori S (2000) Two dioxygenase genes, *Ids3* and *Ids2* from *Hordeum vulgare* are involved in the biosynthesis of mugineic acid family siderophores. Plant Mol Biol **44:** 199–207

Negishi T, Nakanishi H, Yazaki J, Kishimoto N, Fujii F, Shimbo K, Yamamoto K, Sakata K, Sasaki T, Kikuchi S, et al (2002) cDNA microarray analysis of gene expression during Fe-deficiency stress in barley suggests that polar transport of vesicles is implicated is phytosiderophore secretion in Fe deficient barley roots. Plant J **30:** 83–94

Nomoto K, Mino Y, Ishida T, Yoshioka H, Ota N, Inoue M, Takagi S, Takemoto T (1981) X-ray crystal structure of the Copper(II) complex of mugineic acid, a naturally occurring metal chelator of graminaceous plants. J Chem Soc Chem Comm **10:** 338–339

Nozu Y, Tsugita A, Kamijo K (2006) Proteomic analysis of rice leaf, stem and root tissues during growth course. Proteomics **6:** 3665–3670

Ogo Y, Itai RN, Nakanashi H, Inoue H, Kobayashi T, Suzuki M, Takahashi M, Mori S, Nishzawa NK (2006) Isolation and characterization of IRO2, a novel iron-regulated bHLH transcription factor in graminaceous plants. J Exp Bot **57:** 2876–2878

O'Neill MA, Ishii T, Albersheim P, Darvill AG (2004) Rhamnogalacturonan II: structure and function of a borate cross-linked cell wall pectic polysaccharide. Annu Rev Plant Biol **55:** 109–139

Perkins DN, Pappin DJC, Creasey DM, Cotrell JS (1999) Probability-based protein identification by searching sequence databases using mass spectrometry data. Electrophoresis **20:** 3551–3557

Power P, Woods WG (1997) The chemistry of boron and its speciation in plants. Plant Soil **193:** 1–13

Robertson C, Beavis RC (2004) Tandem: matching proteins with mass spectra. Bioinformatics **20:** 1466–1467

Roessner U, Patterson JH, Forbes MG, Fincher GB, Langridge P, Bacic A (2006) An investigation of boron toxicity in barley using metabolomics. Plant Physiol **142:** 1087–1101

Rossignol M, Peltier J, Mock H, Matros A, Maldonado AM, Jorrin JV (2006) Plant proteome analysis: a 2004-2006 update. Proteomics **6:** 5529–5548

Shadforth IP, Dunkley TPJ, Lilley KS, Bessant C (2005) i-Tracker: for quantitative proteomics using iTRAQ. BMC Genomics **6:** 145–150

Suzuki M, Takahashi M, Tsukamoto T, Watanabe S, Matsuhashi S, Yazaki J, Kishimoto N, Kikucho S, Nakanishi H, Mori S, et al (2006) Biosynthesis and secretion of mugineic acid family phytosiderophores in zinc deficient barley. Plant J **48:** 85–97

Takagi S, Nomoto K, Takemoto T (1984) Physiological aspect of mugineic acid, a possible siderophore of graminaceous plants. J Plant Nutr **7:** 469–477

Takano J, Noguchi K, Yasumori M, Kobayashi M, Gajdos Z, Miwa K, Hayashi H, Yoneyama T, Fujiwara T (2002) *Arabidopsis* boron transporter for xylem loading. Nature **420:** 337–340

Takano J, Wada M, Ludewig U, Schaaf G, von Wiren N, Fujiwara T (2006) The Arabidopsis major intrinsic protein NIP5;1 is essential for efficient boron uptake and plant development under boron limitation. Plant Cell **18:** 1498–1509

von Wiren N, Marschner H, Romheld V (1996) Roots of iron-efficient maize also adsorb phytosiderophore-chelated zinc. Plant Physiol **111:** 1119–1125

Wagner Y, Sickmann A, Meyer HE, Daum G (2003) Multidimensional nano-HPLC for analysis of protein complexes. J Am Soc Mass Spectrom **14:** 1003–1011

Washburn MP, Wolters D, Yates III Jr (2001) Large-scale analysis of the yeast proteome by multidimensional protein identification technology. Nat Biotechnol **19:** 242–247

Zieske LR (2006) A perspective on the use of iTRAQ reagent technology for protein complex and profiling studies. J Exp Bot **57:** 1501–1508